A Dynamic Hierarchical Framework for IoT-Assisted Digital Twin Synchronization in the Metaverse

Yue Han, Dusit Niyato, *Fellow, IEEE*, Cyril Leung, *Life Member, IEEE*, Dong In Kim, *Fellow, IEEE*, Kun Zhu, *Member, IEEE*, Shaohan Feng, Xuemin Shen, *Fellow, IEEE*, and Chunyan Miao, *Senior Member, IEEE*

***Abstract*—Metaverse, also known as the Internet of 3-D worlds, has recently attracted much attention from both academia and industry. Each virtual subworld, operated by a virtual service provider (VSP), provides a type of virtual service. Digital twins (DTs), namely, digital replicas of physical objects, are key enablers. Generally, a DT belongs to the party that develops it and establishes the communication link between the two worlds. However, in an interoperable metaverse, data-like DTs can be "shared" within the platform. Therefore, one set of DTs can be leveraged by multiple VSPs. As the quality of the shared DTs may not always be satisfying, in this article, we propose an agile solution, i.e., a dynamic hierarchical framework, in which a group of Internet of Things devices in the lower level are incentivized to collectively sense physical objects' status information and VSPs in the upper level determine synchronization intensities to maximize their payoffs. We adopt an evolutionary game approach to model the devices VSP selections and a simultaneous differential game to model the optimal synchronization intensity control problem. We further extend it as a Stackelberg differential game by considering some VSPs to be first movers. We provide open-loop solutions based on the control theory for both formulations. We theoretically and experimentally show the existence, uniqueness, and stability of the equilibrium to the lower level game and further provide a sensitivity analysis for various system parameters. Experiments show that the proposed dynamic hierarchical game outperforms the baseline.**

***Index Terms*—Crowdsensing, differential game, digital twins (DTs), evolutionary game, game theory, Internet of Things (IoT), metaverse, resource allocation, synchronization.**

Manuscript received 18 March 2022; revised 27 July 2022; accepted 11 August 2022. Date of publication 23 August 2022; date of current version 22 December 2022. This work was supported in part by the Alibaba Group through the Alibaba Innovative Research (AIR) Program and Alibaba-Nanyang Technological University (NTU) Singapore Joint Research Institute (JRI); in part by the National Research Foundation (NRF) and Infocomm Media Development Authority through the Future Communications Research and Development Programme (FCP) through the AI Singapore Programme (AISG) under Grant AISG2-RP-2020-019, through the Energy Research Test-Bed and Industry Partnership Funding Initiative, part of the Energy Grid (EG) 2.0 Programme, through DesCartes and the Campus for Research Excellence and Technological Enterprise (CREATE) programme, and Singapore Ministry of Education (MOE) Tier 1 (RG16/20); and in part by the National Research Foundation of Korea (NRF) Grant funded by the Korean Government (MSIT) under Grant 2021R1A2C2007638 and the MSIT through the ICT Creative Consilience Program under Grant IITP-2020-0-01821 supervised by the IITP. *(Corresponding author: Dong In Kim.)*

Yue Han is with the Alibaba Group and the Alibaba-NTU Joint Research Institute, Nanyang Technological University, Singapore (e-mail: hany0028@e.ntu.edu.sg).

Dusit Niyato and Chunyan Miao are with the School of Computer Science and Engineering, Nanyang Technological University, Singapore (e-mail: dniyato@ntu.edg.sg; ascymiao@ntu.edg.sg).

Cyril Leung is with the Department of Electrical and Computer Engineering, University of British Columbia, Vancouver, BC V6T 1Z4, Canada (e-mail: cleung@ece.ubc.ca).

Dong In Kim is with the Department of Electrical and Computer Engineering, Sungkyunkwan University, Suwon 16419, South Korea (e-mail: dikim@skku.ac.kr).

Kun Zhu is with the College of Computer Science and Technology, Nanjing University of Aeronautics and Astronautics, Nanjing 210016, China (e-mail: zhukun@nuaa.edu.cn).

Shaohan Feng is with the Institute for Infocomm Research, A*STAR, Singapore (e-mail: fengs@i2r.a-star.edu.sg).

Xuemin Shen is with the Department of Electrical and Computer Engineering, University of Waterloo, Waterloo, ON N2L 3G1, Canada (e-mail: sshen@uwaterloo.ca).

Digital Object Identifier 10.1109/JIOT.2022.3201082

I. Introduction

A. Introduction of the Metaverse and Its Economy

THE LONG-TERM global epidemic has dramatically altered people's work and life styles. In-person social gatherings and events have gradually been replaced by various online events, e.g., UC Berkeley held its virtual commencement in 2021 [1] and "Fortnite" organized a virtual concert in 2019, reportedly viewed by 10.7 million people [2]. These virtual events are examples of a computer-mediated virtual environment [3] and can be encapsulated by the concept of the Metaverse, which has been attracting interest from both academia and industry since 2019.

Metaverse has been known as the Internet of 3-D virtual worlds [4]. In fact, it is a platform that hosts various digital subworlds and continues to blur the gap between the physical and the virtual world. Each virtual subworld, operated by a virtual service provider (VSP), offers a specific type of virtual service to Metaverse users, including but not limited to virtual 3-D worlds (e.g., VR chat,[1] virtual safari sightseeing [5], and virtual theme park [6]), nonfungible token (NFT) Games (e.g., Upland),[2] social networking (e.g., virtual conferencing), and augmented reality applications (e.g., immersive training[3] and Pokemon Go).[4] Metaverse users (hereinafter

[1]https://hello.vrchat.com/
[2]https://www.upland.me/
[3]https://www.bizzlogic.com/vrtraining
[4]https://pokemongolive.com/en/

users), represented by avatars, namely, digital replicas of themselves, can have social, immersive, augmented, and interactive experiences in different virtual subworlds with perpetual user accounts [7].

The above-mentioned virtual services may seem similar to the various computer-mediated simulated environments [3], which are created online nowadays. However, the majority of today's simulated environments are developed and operated in a self-governing manner, forbidding a user to access and share digital assets *across* applications, environments, and platforms. For example, it is impossible for a user to transfer his avatar's virtual clothes across Nintendo,[5] Sony's PlayStation Studios,[6] and Microsoft's Xbox Game Studios,[7] as each operates its own engine. In contrast, the Metaverse is known for its interoperability [3], [8], i.e., the standardization based on which the subworlds and games are created. As a result, users can freely access and exchange digital goods among multiple virtual subworlds that are integrated with the Metaverse platform and a VSP can even leverage the existing components in some other virtual subworlds and build its own new subworld to provide its virtual business. The free navigation and access will allow users to experience what they have experienced in the real world in a virtual space and to have even more extraordinary experiences beyond real life. Lite versions of the Metaverse can be seen in the gaming industry now, namely, those cross-platform massively multiplayer online games, such as Roblox,[8] Sandbox,[9] Fortnite,[10] and Axie Infinity.[11] However, the Metaverse is more than gaming and can revolutionize service provisions in all walks of life, e.g., retailing [9], traveling [10], education [11], and social-networking [7].

The two major contributors to the Metaverse economy [12] are the VSPs and users, and Metaverse is dedicated to bringing VSPs and users together and facilitating their interaction and collaboration, i.e., VSP-to-VSP (e.g., digital service combo), VSP-to-user (e.g., digital service provision), user-to-VSP (e.g., remotely offering human intelligence/experience for the tasks offloaded by a VSP), and user-to-user (e.g., socialization and game competition). Both VSPs and users can benefit from the Metaverse platform. For example, a country's tourism board can be a VSP which provides *virtual sightseeing services* [10]. The service includes one-off sensing of the country's tourist attractions, constructing digital replicas of those attractions in the Metaverse, and handling *ad hoc* simulation requests, such as live events (e.g., concerts and festival celebration activities) and social events. As such, even with the country's borders closed due to a pandemic, the country's tourism board (VSP) can still make a profit in the Metaverse. On the other hand, the Metaverse economy benefits the users. For example, users from a foreign country can visit the virtual Universal Studios Hollywood, take a jungle adventure in Yellowstone National Park, and so on, without affected by the global pandemic [13]. It is expected that the Metaverse will provide significant benefits, ultimate conveniences, and new employment opportunities, which will literally transform people's lives in a similar way that the Internet has done.

Notwithstanding its great potential benefits, the Metaverse is still in the nascent stages of its development [12]. One challenge is how to efficiently replicate the real world in the Metaverse [3]. One solution is through synchronization of digital twins (DTs) [14], which are digital replicas of living or nonliving entities in the real world. With DTs, Metaverse users can experience physical entities as if they were interacting with them in the real world, and VSPs can develop businesses based on DTs. An example is virtual driver training [15], in which users are trained on a simulation platform with immersive realistic experience and minimal danger. Here, roads, cars, traffic, commuters and even weather can be replicated on the Metaverse via DTs. Thanks to the Metaverse's interoperability, after being integrated with the Metaverse, those DTs can be additionally integrated into other VSPs' virtual services, such as virtual sightseeing, telemedicine [16] and online route optimization for smart goods delivery [17]. This is because those VSPs may depend on contextual information about the same roads, traffic and weather twin used for the virtual driver training service.

B. Challenges

However, there are five challenges. First, in the era of the Metaverse, all integrated subworlds need to support interoperability. However, in the current budding phase of the Metaverse, we cannot expect that the physical asset owners have already been integrated into the Metaverse. In addition, it cannot be guaranteed that their services have all been transformed into a way that supports interoperability. Therefore, we need to consider some external assistance, e.g., leveraging Internet of Things (IoT) devices, to facilitate the collection of the states information regarding the physical objects, given the asset owners' are not in the Metaverse or do not support the interoperability. Another justification for using additional external assistance of sensing the physical objects' state information is because there can be multiple digital replicas of one physical counterpart in the Metaverse, since a DT can be shared among VSPs due to the interoperability. However, the shared DT may not always meet other VSPs' requirements (e.g., for the freshness of information [18] or the reliability [14]). Those DTs of unsatisfied quality may affect the Quality of Experience (QoE) or Quality of Service (QoS) for those VSPs' virtual businesses. As a result, it is important to have a solution for these VSPs that are not satisfied with the shared DTs, e.g., they can approach to the assistance of external IoT devices to collect additional information on the physical counterparts.

Second, there can be various types of VSPs and can have many ad-hoc requests for additional DTs to augment their virtual businesses. For example, the virtual sightseeing providers may want to include some recent live concerts or seasonal festival celebration activities. Therefore, it can be expensive

[5]https://www.nintendo.com/
[6]https://www.playstation.com/en-sg/corporate/playstation-studios/
[7]https://www.xbox.com/en-US/xbox-game-studios
[8]https://www.roblox.com/
[9]https://www.sandbox.game/en/
[10]https://www.epicgames.com/fortnite/en-US/home
[11]https://axieinfinity.com/

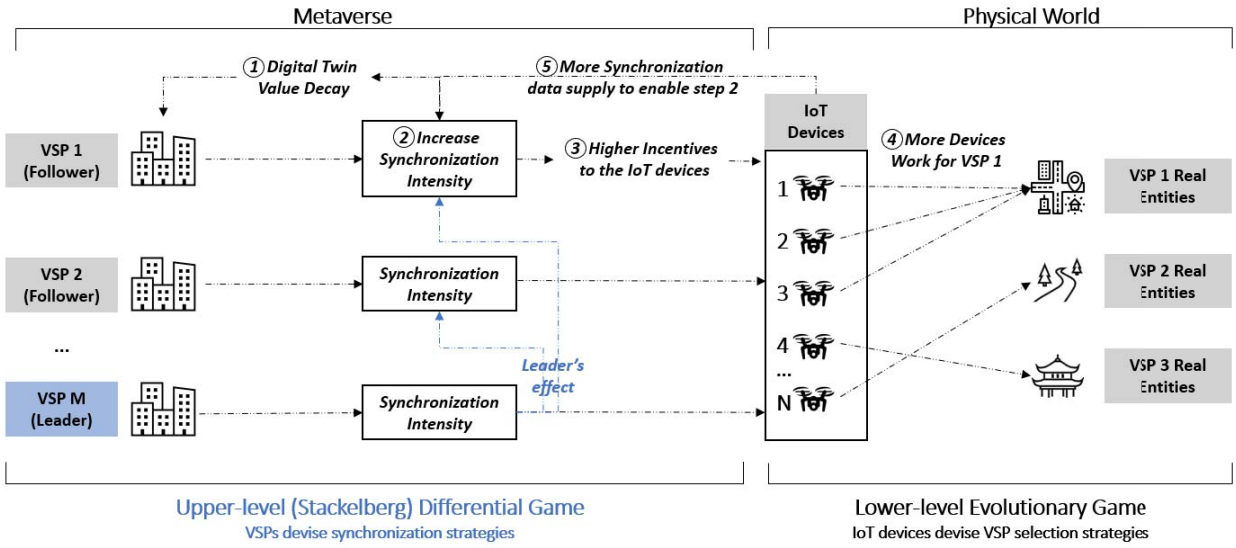

Fig. 1. Dynamic hierarchical framework for IoT-assisted Metaverse synchronization.

and challenging to deploy traditional fixed and static sensors to collect the status data of physical objects. This raises the question of how to leverage a group of *movable* IoT devices to support the agile Metaverse synchronization.

Third, a DT can be associated with some temporal features whose *reliability* decreased with time [14], e.g., temperature or rainfall for a weather twin and traffic volume for a city twin. If there is not enough synchronization between virtual and real worlds, unreliable DTs can affect the outcome of virtual services, such as misjudging a driver's driving skills in an unrealistic environment or a traveler cannot experience what is actually happening in a foreign city at present, making a virtual sightseeing experience less realistic. As the synchronization data (i.e., physical objects states data) are provided by a number of movable IoT devices, an efficient resource allocation solution is needed, so as to efficiently allocate the device resources to match the synchronization intensity required by a VSP.

Forth, it is possible that different VSPs have different levels of tolerance to nonupdated DTs, due to their different business types, the extents to which they use AI, as well as computation capabilities. For example, an nonupdated weather twin may leave little impact on the virtual travel service provider, but a significant impact on virtual driver training by producing a wrong assessment result. A VSP with a stronger AI algorithm deployed and higher computation capacity can predict the patterns of DT states in the near future and, thus, may have higher tolerance to nonupdated DTs. The different tolerance to nonupdated DTs allow VSPs optimize their synchronization intensities differently. Therefore, how to represent, model, and take into account the VSP's tolerance levels in the process of determining the optimal synchronization intensity is critical, which still remains as an open research problem.

Fifth, similar to real-world economics markets, there may be some influential decision makers in the Metaverse market, such as some VSPs with large business volumes. As such, how their decisions about optimal synchronization intensity affect the other following VSPs is not addressed in the literature.

C. Our Contributions

To address the above challenges, in this article, we propose a dynamic hierarchical Metaverse synchronization framework utilizing IoT devices, in which *movable* IoT devices such as drones (unmanned aerial vehicles or UAVs) can collectively sense the current states of the physical counterparts of the VSP's DTs. The system model is shown in Fig. 1 and consists of Metaverse components and Physical World components. In the Metaverse, we treat DT temporal features that influence VSP business profitability as DT values, which subject to natural value decay, i.e., the value naturally drops with time (step ①). As such, it is necessary for VSPs to determine a proper synchronization intensity to maintain DT values without incurring excessive communication, computation, and storage costs due to oversynchronization (step ②). To enable this, the VSPs provide incentives to attract IoT devices to work for them by sensing the corresponding real world entities (step ③). However, faced with different VSPs and their different incentive provisions, an IoT device can independently select a VSP that maximizes its utility and work for it (step ④). After completing the sensing task for the selected VSP, IoT devices transmit the data to the VSP through nearby base stations (step ⑤). With proper cloud processing, VSPs can use synchronization data to update their DTs accordingly, thereby increasing the values of the DTs. In analogous to physical world economic markets, we consider that larger VSPs in the Metaverse may have certain levels of privilege, that is, to determine their synchronization strategies in advance of other smaller VSPs. We refer to a large VSP that moves first as a leader (highlighted in blue in Fig. 1) and smaller VSPs that first observe the leader's synchronization strategies as followers.

We model the above system model as a hierarchical two-level game. The lower level game captures IoT devices'

VSP selection strategies (step ④) as an evolutionary game and the upper level game models VSP synchronization strategy (step ②) as a simultaneous differential game (when no leader exists) and a Stackelberg differential game (in the leader–follower case). The optimal synchronization strategy is solved by the optimal control theory. To summarize, the main contributions of this article are as follows.

1) We propose a novel IoT-assisted synchronization data collection framework by leveraging movable IoT devices to collect physical objects state data. The flexibility of movable devices enables VSPs to have ad-hoc applications and faster virtual business expansion, especially critical for the budding phase of the Metaverse.
2) Due to the self-interested nature and potentially incomplete knowledge of the environment, each device can independently select a VSP to work for, and its decision can be made with only bounded rationality [19]. We adopt a exclusively suitable evolutionary game to capture the device's VSP selection behaviors.
3) We analytically address the optimal synchronization strategies for VSPs by formulating it as a simultaneous differential game and solve it based on the optimal control theory. In particular, we propose DT value dynamics that capture a VSP's level of tolerance to a nonupdated DT. The DT value dynamics as well as the IoT devices' VSP selection dynamics are jointly considered in the system states for the optimal control problem.
4) We further extend the dynamic hierarchical framework by considering leaders and followers among VSPs and formulate it as a differential Stackelberg game. Extensive experiments show that both simultaneous and Stackelberg differential game lead to higher accumulated utility for each VSP, compared to the baseline of a static game.

The remainder of this article is organized as follows. Section II reviews related works. Section III presents the system model and hierarchical dynamic game framework. UAVs' selection of VSPs is formulated as an evolutionary game in Section IV. In Sections V and VI, we formulate the problem as simultaneous differential game and Stackelberg differential game, respectively, to solve for the optimal synchronization strategy. Section VII presents numerical results and sensitivity analysis. Section VIII concludes this article.

II. Related Work

A. Metaverse and Its Architecture

Recently, due to the COVID-19 pandemic restrictions and marketing by leading technology companies, such as Facebook and Microsoft [20], the convenience and usefulness of the virtual world (Metaverse) have been highlighted. Despite some early discussion of the benefits and challenges brought by virtual services in terms of user experiences [7], [9], [11], [21], novel applications in the Metaverse have attract research attention, e.g., Duan *et al.* [12] built a university campus prototype to study social good in the Metaverse, whereas Nguyen *et al.* [22] proposed a Blockchain-based framework for Metaverse applications. An incentive mechanism design for leveraging coded distributed computing for Metaverse services is studied in [23]. In [24], the interconnection of edge intelligence and Metaverse is considered. These examples illustrate the increasing importance of realizing the Metaverse. However, none of them consider how to improve the convergence between the Metaverse and the physical world, in particular, the synchronization intensity problem for VSPs in terms of their DTs. Han *et al.* [25] described an attempt to address this problem, but primarily focus on the VSP selection problem of UAVs without taking into account the synchronization intensity control and temporal values of DTs.

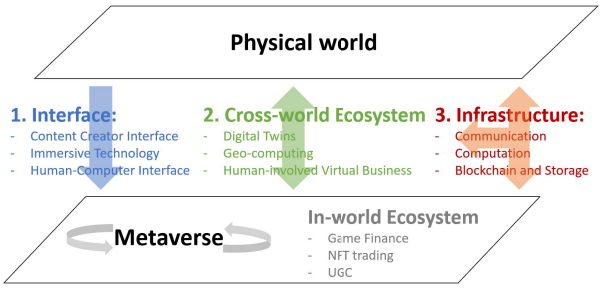

Fig. 2. Four components for the Metaverse [25].

Regarding the Metaverse architecture, there is no consensus, e.g., a seven-layer system [26] and a three-layer architecture [12]. However, based on the Metaverse's functionality, overall, its architecture should include four aspects as shown in Fig. 2: 1) *infrastructure* (the fundamental resources to support the platform, such as communication [27], computation, blockchain [28], and other decentralization techniques); 2) *interface* (immersive technologies, such as AR, VR [15], [29], XR [30], and next generation human-brain interconnection to enrich a user's subjective sense in the virtual life); 3) *cross-world ecosystem* (the services that enable frequent and large amount of data transmission between the Metaverse and the physical world, to enable a *convergence* between the two worlds [31]); and, finally, 4) *in-world ecosystem* (activities that happen only within the virtual world, e.g., transaction of the NFT [32], playing games to earn Crypto (GameFi) [33], and decentralized finance (DeFi) [34]). See [3], [4], [35] for more detailed discussions of the architectures and challenges faced by the Metaverse. Among these four aspects, this article is primarily focused on the cross-world system for the Metaverse, i.e., striving for a convergence of the two worlds.

B. Digital Twins in the Era of Metaverse

DT is not a new concept. They were proposed in 2003 [36] by Grieves in his course on "product life cycle management," which defines DTs by physical product, virtual product, and their connections. Later in 2012, the National Aeronautics and Space Administration (NASA) defined DTs as "integrated multiphysical, multiscale, probabilistic simulations of an as-built vehicle or system using the best available physical models, sensor updates, and historical data" [37]. Although these are early definitions, it is clear that a key feature of DTs is its *mirroring* of physical objects, which means that

continuous updates from physical space to virtual space are needed (physical → virtual), as a physical object's state changes over time.

There is no consensus regarding the updates from DTs to physical objects (virtual → physical). On the one hand, Khan *et al.* [14], Fuller *et al.* [38], and Tao *et al.* [39] believed that there are *bidirectional* updates across cyberspace and physical space for DTs (virtual ↔ physical). To emphasize the bidirectional updates, Fuller *et al.* [38] used *digital models* to refer to the case where there is no update across the two spaces and use *digital shadows* to refer to the case where there is a *one-directional* update from physical space to the cyberspace, i.e., a change in the state of the physical object leads to a change in the digital object and *NOT vice versa*. On the other hand, several other works use DTs as simulation-based only, such as [36], [40], [41]. That is, they treat DTs as digital shadows only (i.e., physical → virtual). Meanwhile, the control of physical assets via their DTs (physical ← virtual) are particularly studied around another concept called cyber–physical systems (CPSs) [42]. CPS can be leveraged to support large distributed control, e.g., automated traffic control and ubiquitous healthcare monitoring and delivery. Given the ambiguity of definitions of DTs, a number of papers have already called for more precise clarity on the difference between the DTs, the digital shadows, and the CPS [14], [38].

In contrast to the DT studies in the literature, in this article, we just use the term DTs to refer to the *digital existence in the Metaverse*, which is a digital replication of a physical object. The reasons for loosening the definition of DTs are as follows. First, compared to smart manufacturing or Industry 4.0 in which DTs are created and studied merely for a particular type of application [39] owned by a company, the Metaverse, with a platform feature, can support different kinds of virtual businesses [3]. Therefore, one DT can be used by various VSPs. If all these VSPs have bidirectional communication between the physical and the cyber space, and each VSP has its own change in its DTs, then it can be confusing about which VSP's DT state change should be synchronized with the physical counterpart. Hence, we do not consider the complex case regarding bidirectional communication and uncertain DT ownership in an interoperable Metaverse. Second, many brand new application scenarios are expected to emerge in the Metaverse. This is because the interoperability [8] (e.g., sharing of DTs among VSPs), human experience being important in the virtual services [43], and the maturity of blockchain and artificial intelligence [22]. For example, the combination of NFT and DTs is considered to be the next step of NFT [32], in which the value of an NFT is attached to a physical asset and the change of the asset's state affects the value of the NFT. Our loose definition of DT can, therefore, be suited to more types of applications in the Metaverse by leveraging the external assistance of IoT for sensing the states of real entities.

III. System Model and Problem Formulation

We consider a network that consists of: 1) N edge devices (e.g., UAVs) represented by the set $\mathcal{N} = \{1, \ldots, n, \ldots, N\}$ and 2) M VSPs represented by the set $\mathcal{M} = \{1, \ldots, m, \ldots, M\}$, as shown in Fig. 1. An element of the set $\mathcal{M}$ and $\mathcal{N}$ is represented by m and n, respectively. We consider UAVs as the IoT devices hereafter.

Each of VSPs uses a set of DTs that are critical to its virtual business profit. As the dissimilarity between a DT and its psychical counterpart increases with time, it is expected that the value of a DT to a VSP's virtual business decays with times naturally. Let $\theta_m > 0$ represent the value decay rate of the DTs of VSP m. We consider that the different VSPs may have different DT value decay rates, possibly due to, e.g., the types of their virtual services, computational capabilities, and the extents to which they use AI.[12]

Let $z_m(t) \geq 0$ denote the DT value status, representing the utility that a DT brings to VSP m at time instant t. Based on the linear utility model [45], [46], we model the rate of change for the DT values, which is the first-order time derivative $\dot{z}_m(t) = \mathrm{dz(t)/dt}$ as follows:

$$\dot{z}_m(t) = \eta_m(t) - \theta_m z_m(t), \quad m \in \mathcal{M} \tag{1}$$

where $\eta_m(t)$ denotes the intensity, or rate, at which the synchronization activities are carried at time t. One can interpret the DT value dynamics in (1) as follows: if VSP m determines not to synchronize DTs at all, i.e., $\eta_m(t) \equiv 0$, then the value of DTs deteriorates at the (time independent) rate θ_m. By using a positive rate of synchronization, i.e., $\eta_m(t) > 0$, the VSP can slow down, or even reverse, the process of deterioration of its DTs.[13] To simplify, we use $\boldsymbol{z}(t) = [z_m(t)]_{m\in\mathcal{M}}$ to denote the vector of DT values of all VSPs and let the vector $\boldsymbol{\eta}(t) = [\eta_m(t)]_{m\in\mathcal{M}}$ denote the synchronization strategies of all VSPs at each instant t.

To synchronize DTs with their real counterparts, the states data of the real counterparts are needed. Here, we consider a set of N UAVs can be motivated to assist VSPs synchronization tasks by sensing the corresponding real entities states for the VSPs. Here, for simplicity, we consider a group of UAVs with the same type, e.g., characterized by the same sensing quality and unit energy cost [47]. The extension to the scenario with heterogeneous types of UAVs is straightforward, as the set of UAVs can always be partitioned into multiple subpopulations so that the UAVs within a subpopulation are of the same type.

Based on synchronization requests from M VSPs, each of the N UAVs can select a VSP to work for. UAVs that select the same VSP are expected to collectively sense the real entities of interest to the VSP and share the incentives provided by the VSP. It is expected that when VSP m's synchronization intensity increases, VSP m will allocate more incentives to motivate UAVs to work for it. As such, the total incentive pool from VSP m should be positively correlated with the synchronization intensity chosen by VSP m.

In summary, the synchronization intensity $\eta_m(t)$ affects the values of its own DTs as well as the percentage of UAVs

[12]For example, a VSP with a stronger AI algorithm and higher computation capacity may have lower value decay rates, since with the adoption of AI, VSPs can study the historical state data obtained from the physical counterparts and adjust the status of DTs based on the predictable pattern trained with AI, thereby maintaining the reliability of the DTs [44].

[13]A waste of resources due to over synchronization is considered in the penalty term in the utility function. See Section V-A for details.

that sense the physical twins to provide synchronization data (UAV's VSP selection distribution). Since the synchronization intensity is controlled by the VSP, we also refer to it as *a control variable, a control, or a strategy* for a VSP, which is a function of the time t. By determining an optimal control strategy on the synchronization intensity, the VSP can affect the states of the system, including DT value states in addition to the UAV's VSP selection strategy, thereby optimizing the utility for the VSP.

To identify the optimal control strategy of the synchronization intensity and its associated DT values and the UAV's VSP selections, our study focuses on a dynamic hierarchical framework as follows.

1) *Lower Level Evolutionary Game:* At the lower level, we investigate VSP selection strategies for UAVs. Every UAV is considered to have bounded rationality, that is, to select a strategy that is satisfactory rather than optimal [19]. This is to counter the case that UAV decisions are suboptimal with the potentially incomplete information of the game (e.g., the payoffs received by other UAVs), especially when the number of UAVs is large. In this regard, we formulate the problem as an evolutionary game in Section IV, which models the strategy adaptation process of the UAVs.
2) *Upper level (Stackelberg) Differential Game*: At the upper level, we investigate the optimal synchronization strategies of the VSPs. As the synchronization intensity jointly affects the synchronization data supply and the value status of the DTs, the VSPs need to devise the optimal control strategy about synchronization intensity so that the accumulated utilities discounted at the present time are maximized. We adopt a differential game approach to solve the problem in Section V. Additionally, when there is an influential VSP in the Metaverse market that has the privilege of determining strategy first, we formulate the problem as a Stackelberg differential game and solve it based on the control theory.

The notations used in this article are presented in Table I. Arguments to a function, e.g., time variable t, may be omitted from expressions when there is no ambiguity. The notation of $:=$ means "defined to be equal to."

TABLE I
NOTATIONS USED IN THE SYSTEM MODEL

Notation	Description
	Section III
$m \in \mathcal{M}$	index of a VSP, $\lvert\mathcal{M}\rvert = M$
$n \in \mathcal{N}$	index of a UAV, $\lvert\mathcal{N}\rvert = N$
$\eta_m(t), \boldsymbol{\eta}$	synchronization intensity of VSP m, vector of $[\eta_m]_{m\in\mathcal{M}}$
$z_m(t), \boldsymbol{z}$	values of DTs of VSP m, vector of $[z_m]_{m\in\mathcal{M}}$
θ_m	time-independent value decay parameters for VSP m
$\mathcal{T}$	Time horizon $\mathcal{T} = [0, T]$
	Section IV
$x_m(t)$	percentage of UAVs selecting VSP m at time t
$\boldsymbol{x}$	vector of $[x_m]_{m\in\mathcal{M}}$
$u_m(\boldsymbol{x}, \eta_m)$	utility of UAVs selecting VSP m
d_m	number of DTs for VSP m
$g(\cdot)$	weighting function used in the incentive pool
$R_m(t)$	incentive pool for the VSP m
c_m	cost of UAVs in assisting VSP m for synchronization
$\bar{u}$	average utility of the UAVs
δ	learning rate
	Sections V and VI
b	average data contribution from each UAVs
α_m	unit data price for VSP m
β_m	VSP preference of a unit increase in DTs values
v_m	VSP preference of the values of the DTs
k_m	average data size request rate
ω_m^i	weights in J_m, $i = 1, 2, 3, 4$
ρ	discounting factor
J_m	instantaneous utility function of VSP m
J_m^i	components for the J_m, $i = 1, 2, 3, 4$
$\mathfrak{J}_m$	the objective function for the VSP m
H_m	Hamiltonian function of VSP m
H_m^*	Maximized Hamiltonian function of VSP m

IV. LOWER LEVEL EVOLUTIONARY GAME FOR UAVS' VSP SELECTION STRATEGIES

In this section, to describe the bounded rationality of the UAVs and dynamics of UAVs' VSP selection strategy adaptation, we adopt the evolutionary game with replicator dynamics. The UAV owner's utility model and replicator dynamics are introduced in Section IV-A. Then, in Section IV-B, we prove the existence, uniqueness, and stability of the lower level evolutionary game.

A. Evolutionary Game Formulation

Evolutionary game is formulated based on a set of populations with evolutionary dynamics. The various aspects of the evolutionary game are as follows.

1) *Players and Populations:* Each UAV $n \in \mathcal{N}$ is a player of the evolutionary game. In addition, the set $\mathcal{N}$ is referred to as the population of players.
2) *Strategy:* The VSP selection is a pure strategy that can be implemented by the player.
3) *Population States:* Population state is the strategy distribution for the population, denoted by a vector $\boldsymbol{x}(t) = [x_m(t)]_{m\in\mathcal{M}}$. The component $x_m(t)$ denotes the percentage of UAVs in the population that select VSP m at the time instant t. As the population states are subject to $\sum_{m\in\mathcal{M}} x_m(t) = 1$ and, therefore, the state space, i.e., the set of all the possible population states, is a unit simplex $\Delta \in \mathbb{R}^{M-1}$.
4) *Utility Functions:* Utility function $u_m(\boldsymbol{x}(t), \eta_m)$ describes the utility that a UAV can receive given the population states $\boldsymbol{x}(t)$ and the synchronization strategy η_m.

Each VSP m has d_m DTs and chooses the synchronization intensity as $\eta_m(t)$, where $\eta_m(t) \geq 0$, at time t. Let the time horizon for the analysis be defined as $\mathcal{T} = [0, T]$. We refer to $\boldsymbol{\eta}(t)$, $t \in \mathcal{T}$, as the control path over the time horizon $\mathcal{T}$. We omit time variable t for simplicity if there is no confusion. Note that determination of the optimal synchronization strategy path over $\mathcal{T}$ can be further explored as an optimal control problem, which is to maximize the present value of the accumulated utility that the VSP can obtain. The extension is in Section V. In this section, we assume that the optimal synchronization intensity path has been determined by the VSPs.

For VSP m, the incentive pool that it allocates to its associated UAVs is given as follows:

$$R_m(t) = \eta_m(t) d_m g(\theta_m) \tag{2}$$

where $g(\cdot)$ is a monotonically increasing function representing the weight affected by the value decay rate θ_m. One can interpret (2) as both synchronization rate η_m and the number of DTs d_m have a positive correlation with the incentive pool. That is, the higher the synchronization intensity or the number of DTs that a VSP has, the more incentives the VSP should offer UAVs. Similarly, the higher the decay rate θ_m is, the more incentives a VSP should offer. We consider an affine mapping for $g(\cdot)$, e.g., $g(\theta_m) = g_0 + g_1\theta_m$, where g_1 is a positive number to represent such a positive correlation between the decay rate and the incentive.

Given the population states $\boldsymbol{x}$, there are Nx_m UAVs that select VSP m to sense the data and assist its synchronization tasks. With a uniform incentive sharing scheme [25], each UAV can obtain the incentives with amount $([R_m(t)]/[Nx_m(t)])$. Let c_m represent the energy cost incurred by the sensing task for VSP m, e.g., UAV's energy cost flying from the base to the target region and the communication cost [48]. The utility received by a UAV that selects VSP m is as follows:

$$u_m(\boldsymbol{x}, \eta_m) = \frac{R_m(t)}{Nx_m(t)} - c_m = \frac{\eta_m(t) d_m g(\theta_m)}{Nx_m(t)} - c_m. \tag{3}$$

The utility information for selecting each of the VSPs at the current time t can be exchanged among UAVs, e.g., at their base or device-to-device (D2D) communication in the air. As such, the UAV may adjust its VSP selection strategy at time $t+1$. The evolutionary process of the VSP selection strategy can be modeled by *replicator dynamics* [19], which is a set of ordinary differential equations, given as follows:

$$\dot{x}_m = \delta x_m(u_m - \bar{u}), \quad m \in \mathcal{M} \tag{4}$$

where δ is the learning rate of the UAVs, $\dot{x}_m := dx_m(t)/dt$, and $\bar{u} := \sum_{m\in\mathcal{M}} x_m u_m$ denotes the average utility that a UAV population can have. Again, we omit arguments in $u_m(\boldsymbol{x}(t), \eta_m)$, and $x_m(t)$ for simplicity.

It can be seen from (4) that the population state $\boldsymbol{x}_m(t)$ evolves when the payoff received by a UAV is different from the population average utility. If the reward received by a device that selects VSP m is higher than the average utility, i.e., $u_m > \bar{u}$, then the population state $x_m(t)$ increases since more UAVs adapt their strategies and select VSP m, i.e., $\dot{x}_m > 0$. The evolutionary process stops when $\dot{x}_m = 0$ for all $m \in \mathcal{M}$. This is called the *stationary state* or evolutionary equilibrium (EE). The stationary states can be achieved by either $x_m = 0$ for all VSP except one or $u_m = \bar{u}\ \forall u \in \mathcal{M}$. The former leads to a set of *boundary stationary points* [19], [49] lying on a vertex of Δ and the latter leads to a set of *interior stationary points*. Next, we prove that the EE uniquely exists for the lower level evolutionary game, and is evolutionarily robust as well.

B. Existence, Uniqueness, and Stability of EE

Since the payoff is affected by the synchronization strategy $\eta_m(t)$ adopted by the VSP m, the evolution of a population state described by the replicator dynamics is subject to the controls of VSPs. The following theorem discusses the existence and uniqueness of the solution under these controls.

Theorem 1: For the dynamical system defined in (4) with initial condition $\boldsymbol{x} = \boldsymbol{x}_0$, there exists a unique solution $\boldsymbol{x}(t)$ defined for all $t \in [0, T]$.

The proof is given in Appendix A. After we prove that the solution $\boldsymbol{x}(t)$ exists, given the initial state $\boldsymbol{x}_0$, conditioned on any control from VSPs, we now show that the solution is *asymptotically stable*. According to [19], if no small perturbation of the state induces a movement away from it then the state is called *Lyapunov stable*. The state is *asymptotically stable* if 1) it is Lyapunov stable and 2) all sufficiently small perturbations induce a movement back toward the state. It is straightforward to examine that the boundary stationary points are unstable [49]. Therefore, we only examine interior stationary points.

Theorem 2: For a single UAV population, the interior stationary points of the dynamical system (4) are asymptotically stable.

The proof is given in Appendix B. See [50] for the details of the implementation of an algorithm to find the ESS with the evolutionary dynamics.

V. Upper Level Differential Game for Simultaneous Decision-Making VSPs

In the upper level, we need to solve the optimal control problem regarding the synchronization intensity given the population state dynamics in (4) and the value dynamics in (1). In this section, we consider the problem in which all VSPs are simultaneous decision makers in the game, and formulate the problem as a simultaneous differential game in Section V-A. We adopt the open-loop Nash equilibrium as the solution to this game in Section V-B.

A. Problem Formulation for the Simultaneous Move

We consider that the M VSPs choose their synchronization strategies at the same time, and each player competes to maximize the objective functional $\mathfrak{J}_m$, i.e., the present value of utility derived over a finite or infinite time horizon, by designing a synchronization strategy η_m that is under the VSP's control. The choice of synchronization intensity by a player, say VSP m, influences: 1) the evolution of the UAV population states $\boldsymbol{x}(t)$; 2) the value states of the DT $z_m(t)$; and 3) the objective functional of the other VSPs in the set $\mathcal{M}$, i.e., $\mathfrak{J}_{m'}$, $m' = 1, 2, \ldots, m-1, m+1, \ldots, M$. The influence to: 1) and 2) is captured via a set of differential equations (the system dynamics). The derivation of $\mathfrak{J}_m$ is given as follows.

With $x_m(t)N$ UAVs assisting VSP m in sensing the current states of its real world twins and $z_m(t)$ being the current values of its DTs, the current utility rate J_m at time t for VSP m can be described as follows:

$$J_m(\boldsymbol{x}, \boldsymbol{z}, \boldsymbol{\eta}, t) = \omega_m^1 J_m^1 + \omega_m^2 J_m^2 - \omega_m^3 J_m^3 - \omega_m^4 J_m^4 \tag{5}$$

where

$$J_m^1 = x_m N b \alpha_m, \quad J_m^2 = \beta_m z_m d_m \tag{6}$$
$$J_m^3 = (z_m - v_m)^2, \quad J_m^4 = (x_m N b - \eta_m d_m k_m)^2. \tag{7}$$

That is, J_m can be interpreted as the weighted sum of four utility components J_m^1, J_m^2, J_m^3, and J_m^4, in which J_m^1 and J_m^2 are the positive utility, and J_m^3 and J_m^4 are the disutility. $\omega_m^i \geq 0, i = \{1, 2, 3, 4\}$ are the weight parameters to form the objective function J_m. We explain the utility component as follows.

1) J_m^1: It represents the gains generated by the acquisition of new data of the size $x_m N b$, where b represents the average amount of data that a UAV transmits to a VSP. Here, with synchronization data from the UAVs, VSP as a data supplier to the Metaverse platform, can benefit by selling the data to the Metaverse platform. The platform, as an intermediary to provide the data interoperability, can benefit the other VSPs to construct the DTs for their own use. Therefore, there is a portion of revenue inflow for VSP m that is linked to the data supply, or the data contribution from the UAVs. Let α_m denote the unit data price for the VSP m, then we have $J_m^1 = \alpha_m x_m N b$ in (6).
2) J_m^2: It represents the gains (e.g., virtual business profit) generated by the DTs with value of z_m. Here, we consider that the business is positively correlated with the DTs values. Therefore, the gains can be evaluated as $J_m^2 = \beta_m z_m d_m$, where β_m denotes the unit preference value that VSP m has toward a unit increase in the value of the DTs. In addition, β_m is considered to concave-upward with respect to θ_m, e.g., $\beta_m = e^{10\theta_m}$. This is to indicate DTs are valued more when the VSP is more sensitive to the nonupdated DTs, i.e., a higher valued decay rate.
3) J_m^3: It represents a penalty term, reflecting disutility when DT values are far away from the preferred values, e.g., the twins are not fresh enough (undersynchronized) or too fresh than what is needed (oversynchronized, leading to excessive synchronization cost). Let v_m denote the VSP's desired values of its DTs, and J^3 can be defined as $(z_m - v_m)^2$ accordingly [51].
4) J_m^4: It represents the disutility caused by UAVs' insufficient data supply. As mentioned before, d_m is the number of DTs of VPS m. With the synchronization intensity η_m, overall, the total amount of data that VSP m requires from the UAVs devices is $d_m \eta_m k_m$, where k_m is the average unit data request rate of the DT. However, since there are $x_m N$ devices that choose VSP m, the total data contribution to VSP m is $x_m N b$ as stated earlier. The gap of $(d_m \eta_m k_m - x_m N b)$ results in disutility to the VSP m. For example, when an insufficient number of UAVs select VSP m, UAVs can complete the synchronization task at lower sampling rates [52], resulting in lower quality synchronization data and affecting the utility of the VSP m. We adopt the square term to prevent the data from being overcontributed as well.

The objective functional $\mathfrak{J}_m(\boldsymbol{\eta})$ to be maximized for VSP m is defined by the discounted cumulative payoff over the time horizon $\mathcal{T}$, expressed as follows:

$$\begin{aligned}\mathfrak{J}_m(\boldsymbol{\eta}) &= \int_0^T e^{-\rho t} J_m(\boldsymbol{x}(t), \boldsymbol{z}(t), \boldsymbol{\eta}(t), t)\, \mathrm{d}t \\ &= \int_0^T e^{-\rho t} \Big\{ \omega_m^1 x_m(t) N b \alpha_m + \omega_m^2 z_m(t) \beta_m - \omega_m^3 \\ &\qquad (z_m(t) - v_m)^2 - \omega_m^4 [x_m(t) N b - \eta_m(t) d_m k_m]^2 \Big\}\, \mathrm{d}t \end{aligned} \tag{8}$$

where $\rho \geq 0$ denotes the constant time preference rate (or discount rate) for VSPs. $J_m(\boldsymbol{x}(t), \boldsymbol{z}(t), \boldsymbol{\eta}(t), t)$ is the instantaneous utility derived by choosing the synchronization intensity value $\boldsymbol{\eta}(t)$ at time t when the current states of the game is $\boldsymbol{x}(t)$ and $\boldsymbol{z}(t)$, as explained earlier in (5).

Therefore, the optimal synchronization intensity control problem for VSP m can be formulated as

$$\max_{\eta_m} \ \mathfrak{J}_m(\boldsymbol{\eta}) \tag{9}$$
$$\text{s.t.} \ \ \dot{x}_m(t) = \delta x_m(t)(u_m(t) - \bar{u}(t)) \quad \forall m \in \mathcal{M} \tag{10}$$
$$\dot{z}_m(t) = \eta_m(t) - \theta_m z_m(t) \quad \forall m \in \mathcal{M} \tag{11}$$
$$\boldsymbol{x}(0) = \boldsymbol{x}_0, \quad \boldsymbol{z}(0) = \boldsymbol{z}_0 \tag{12}$$
$$\boldsymbol{x}(t) \in \Delta, z_m(t) \geq 0, \eta_m(t) \geq 0 \tag{13}$$

for $m = 1, 2, \ldots, M$, where column vectors $\boldsymbol{x}(0)$ and $\boldsymbol{z}(0)$ are initial states for the population states of UAVs and VSPs of DT values.

B. Open-Loop Nash Solution

A *Nash solution* or Nash equilibrium is an M-tuple of synchronization strategies $\boldsymbol{\eta} = [\eta_1, \eta_2, \ldots, \eta_M]$ such that, given the opponents' equilibrium synchronization strategies, no VSP has an incentive to change its own strategy. Denote the synchronization strategies of VSPs other than m as $\boldsymbol{\eta}_{-m} := [\eta_1, \eta_2, \ldots, \eta_{m-1}, \eta_{m+1}, \ldots, \eta_M]$. In the differential game, the Nash solution is defined by a set of M admissible trajectories $\boldsymbol{\eta}^* := [\eta_1^*, \eta_2^*, \ldots, \eta_M^*]$, which have the property that

$$\mathfrak{J}_m(\boldsymbol{\eta}^*) = \max_{\eta_m} \mathfrak{J}_m(\eta_1^*, \ldots, \eta_{m-1}^*, \eta_m, \eta_{m+1}^*, \ldots, \eta_M^*) \tag{14}$$

for $m = 1, 2, \ldots, M$.

Next, we adopt the *open-loop solutions* for the above Nash differential game. The open-loop Nash solution to the optimal control problem refers to the case where the control paths are functions of time t only, satisfying (14). For simplicity, hereafter, we use a column vector $\boldsymbol{y}$ to represent the system states $\boldsymbol{x}$ and $\boldsymbol{z}$, i.e., $\boldsymbol{y} = [x_1, x_2, \ldots, x_M, z_1, z_2, \ldots, z_M]^T$. Then, the constraints defined in (10)–(13) can be replaced by the following conditions:

$$\dot{\boldsymbol{y}}(t) = [\dot{x}_1, \ldots, \dot{x}_M, \dot{z}_1, \ldots, \dot{z}_M]^\top \tag{15}$$
$$\boldsymbol{y}(0) = \left[\boldsymbol{x}(0)^\top, \boldsymbol{z}(0)^\top\right]^\top \tag{16}$$
$$\boldsymbol{y}(t) \in \mathcal{Y} := \Delta \times \mathbb{R}_+^M, \quad \eta_m(t) \in \mathbb{R}_+. \tag{17}$$

This means that the process to solve the open-loop Nash solution is to solve the optimal control problem $\mathscr{P}1$ defined by

$$\max_{\eta_m} \ \mathfrak{J}_m(\eta_m, \boldsymbol{\eta}_{-m}^*)$$
$$\text{s.t.} \ \ (15) - (17) \tag{18}$$

for $m = 1, 2, \ldots, M$. To solve $\mathscr{P}1$, we first define a (current-value) Hamiltonian function H as follows:

$$H_m(\boldsymbol{y}, \eta_m, \boldsymbol{\lambda}_m, t) = J_m\big(\boldsymbol{y}, \eta_m, \boldsymbol{\eta}^*_{-m}, t\big) + \boldsymbol{\lambda}_m \dot{\boldsymbol{y}} \tag{19}$$

for $m = 1, 2, \ldots, M$. The domain of H_m is the set $\{(\boldsymbol{y}, \eta_m, \boldsymbol{\lambda}_m, t) | \boldsymbol{y} \in \mathcal{Y}, \eta_m \in \mathbb{R}_+, \boldsymbol{\lambda}_m \in \mathbb{R}^{2M}, t \in \mathcal{T}\}$. Here, the row vector $\boldsymbol{\lambda}_m = [\lambda_{m1}, \lambda_{m2}, \ldots, \lambda_{m2M}]$ is called the (current-value) adjoint variable or costate variables. Therefore, the maximized Hamiltonian function $H^* : \mathcal{Y} \times \mathbb{R}^{2M} \times \mathcal{T} \to \mathbb{R}$ is

$$H^*_m(\boldsymbol{y}, \boldsymbol{\lambda}_m, t) = \max\{H_m(\boldsymbol{y}, \eta_m, \boldsymbol{\lambda}_m, t) | \eta_m \geq 0\}. \tag{20}$$

A necessary and sufficient condition for the optimal control is given by the augmented maximum principle, stated as in Theorem 3 (see [53] for the detailed proof).

Theorem 3: Consider an optimal control problem $\mathscr{P}1$ and define the Hamiltonian function H_m and the maximized Hamiltonian function H^*_m as above. The state space Θ is a convex set and the scrap value function S is continuously differentiable and concave (note that $S \equiv 0$ in $\mathscr{P}1$). If there exists an absolutely continuous function $\boldsymbol{\lambda}_m : [0, T] \to \mathbb{R}^{2M}$ for all $m \in \mathcal{M}$, such that the maximum condition

$$H_m\big(\boldsymbol{y}, \eta^*_m, t\big) = H^*_m(\boldsymbol{y}, \boldsymbol{\lambda}_m, t) \tag{21}$$

the adjoint (costate) equation

$$\dot{\boldsymbol{\lambda}}_m = \rho \boldsymbol{\lambda}_m - \frac{\partial H^*_m(\boldsymbol{y}, \boldsymbol{\lambda}_m, t)}{\partial \boldsymbol{y}} \tag{22}$$

and the transversality condition

$$\boldsymbol{\lambda}_m(T) = S'(\boldsymbol{y}(T)) = 0 \tag{23}$$

are satisfied, and such that the function H^*_m is concave and continuously differentiable with respect to x for all $t \in \mathcal{T}$, then $\eta_m(\cdot)$ is an optimal control path. If further the set of feasible controls does not depend on $\boldsymbol{y}$ (which is true for $\mathscr{P}1$ as $\eta_m \in \mathbb{R}_+$), (22) can be replaced by

$$\dot{\boldsymbol{\lambda}}_m = \rho \boldsymbol{\lambda}_m - \frac{\partial H_m\big(\boldsymbol{y}, \eta^*_m, t\big)}{\partial \boldsymbol{y}}. \tag{24}$$

Note that $\partial H_m(\boldsymbol{y}, \eta^*_m, t)/\partial \boldsymbol{y}$ is a row vector, following [54] that the derivative of a real-valued function with respect to a vector (no matter a column vector or a row vector) is a row vector. Furthermore, to solve (21), we note that the function H_m in $\mathscr{P}1$ is strictly concave with respect to η_m. Therefore, we can instead solve η^*_m by the first-order optimality conditions, given as follows:

$$\left.\frac{\partial H_m(\boldsymbol{y}, \eta_m, t)}{\partial \eta_m}\right|_{\eta_m = \eta^*_m} = 0. \tag{25}$$

After η^*_m is solved by (25), a boundary value problem of a system of ordinary differential equations can be defined by $\dot{\boldsymbol{y}}$ in (15), $\dot{\boldsymbol{\lambda}}$ in (24), together with their boundary values defined in (16) and (23). The states for this new dynamic systems are $\boldsymbol{y}$ and $\boldsymbol{\lambda}$, which can be numerically solved using *bvp4c* in MATLAB, or *scipy.integrate.solve_bvp* in python.

VI. Upper Level Differential Game for VSPs With Hierarchical Decision Making Process

After obtaining the solution for the simultaneous play VSPs in Section V, we now consider a more complicated realistic case, in which some VSPs are allowed by the Metaverse to choose their synchronization strategies earlier than the other VSPs. We refer to such VSPs as *leaders*. The VSPs that observe leaders' strategies and then make their decisions are called *followers*. To model this sequential strategic interaction among the VSPs, or a hierarchical play, we adopt the Stackelberg differential game.

A. Problem Formulation

We use $\mathcal{L}$ to denote the set of leaders and $\mathcal{F}$ the set of followers, such that $\mathcal{L} \cap \mathcal{F} = \emptyset$ and $\mathcal{L} \cup \mathcal{F} = \mathcal{M}$. We use $\boldsymbol{\eta}^L = [\eta^L_i]_{i \in \mathcal{L}}$ to denote synchronization strategy of leaders and $\boldsymbol{\eta}^F = [\eta^F_m]_{m \in \mathcal{F}}$ synchronization strategy of followers, so as $\boldsymbol{\eta}^{L*}$ and $\boldsymbol{\eta}^{F*}$ for the optimal ones. At time 0, the leaders announce the synchronization strategy path $\boldsymbol{\eta}^L(t)$. The followers, taking those synchronization strategy paths as given, choose their synchronization strategies $\boldsymbol{\eta}^F(t)$ so as to maximize their objective functional.

1) Followers' Problem $\mathscr{P}_F$: Given the leader's optimal synchronization strategy paths $\boldsymbol{\eta}^L$, the followers problem $\mathscr{P}_F$, is the same as $\mathscr{P}_1$ defined in Section V. In particular, for a follower $m \in \mathcal{F}$, the optimal control problem is

$$\begin{aligned} \max_{\eta^F_m} \quad & \mathfrak{J}_m\Big(\eta^F_m, \boldsymbol{\eta}^L, \eta^{F*}_{\mathcal{F}\setminus\{m\}}\Big) \\ \text{s.t.} \quad & (15) - (17) \end{aligned} \tag{26}$$

where $\mathcal{F} \setminus m := \{i \in \mathcal{F}, i \neq m\}$ is the set of followers other than VSP m. For the follower $m \in \mathcal{F}$, its Hamiltonian function, denoted by H^L_m, is the same as (19), that is $H^L_m = H_m$. Then, the optimal synchronization strategy η^{F*}_m for the follower m is equivalent to η^*_m, which is the solution to (25), and adjoint equations $\dot{\boldsymbol{\lambda}}_m$ satisfies (24). Due to the strict concavity of H^F_m, η^{F*}_m can be uniquely determined by (25), as a function of $\boldsymbol{y}$, $\boldsymbol{\eta}^L$, $[\eta^{F*}_j]_{j \in \mathcal{F}\setminus m}$ and t, for all $m \in \mathcal{F}$. That is, we can write

$$\eta^{F*}_m = \tilde{\mathsf{g}}_m\Big(\boldsymbol{y}, \boldsymbol{\lambda}_m, \boldsymbol{\eta}^L, \boldsymbol{\eta}^{F*}_{\mathcal{F}\setminus\{m\}}, t\Big) \quad \forall m \in \mathcal{F} \tag{27}$$

which can be further simplified by substituting $[\eta^{F*}_j]_{j \in \mathcal{F}\setminus m}$ based on (27) into $\tilde{\mathsf{g}}_m(\cdot)$. Therefore, we can express η^{F*}_m as a function of $\boldsymbol{y}, \boldsymbol{\lambda}_m$, and $\boldsymbol{\eta}^L$ as follows:

$$\eta^{F*}_m = \mathsf{g}_m\big(\boldsymbol{y}, \boldsymbol{\lambda}_m, \boldsymbol{\eta}^L, t\big) \quad \forall m \in \mathcal{M} \tag{28}$$

or the vector function $\boldsymbol{\eta}^{F*} = \mathsf{g}(\boldsymbol{y}, \Lambda, \boldsymbol{\eta}^L, t)$, where $\Lambda := [\boldsymbol{\lambda}_m]_{m \in \mathcal{F}}$ represents all the adjoint (costate) variables in $\mathscr{P}_F$.

Substituting (28) into (24), we obtain

$$\dot{\boldsymbol{\lambda}}_m = \rho \boldsymbol{\lambda}_m - \frac{\partial H_m\big(\boldsymbol{y}, \mathsf{g}_m\big(\boldsymbol{y}, \boldsymbol{\lambda}_m, \boldsymbol{\eta}^L, t\big), t\big)}{\partial \boldsymbol{y}}, \quad m \in \mathcal{F}. \tag{29}$$

Equations (15)–(17), (23), (28), and (29) characterize the follower's best response to the leaders control path $\boldsymbol{\eta}^{L*}$.

2) Leaders' Problem $\mathscr{P}_L$: As for the leaders' problem $\mathscr{P}_L$, for any leader $i \in \mathcal{L}$, it knows the followers' best responses. Therefore, different from the simultaneous differential game, the system dynamics additionally include the adjoint equations of the followers' problem. Again, similar to the follower's game, among leaders, we obtain the Nash equilibrium. As such, given the best responses of all the followers, and the other opponent leaders play their strategy $\boldsymbol{\eta}^L_{\mathcal{L}\setminus i}$, the optimal control problem for the leader $i \in \mathcal{L}$ is formulated as follows:

$$\begin{aligned} \max_{\eta_i^L} \ & \mathfrak{J}_i\left(\eta_i^L, \boldsymbol{\eta}^{F*}, \boldsymbol{\eta}^L_{\mathcal{L}\setminus\{i\}}\right) \\ \text{s.t.} \ & (15)-(17),\ (23),\ (29),\ (28) \end{aligned} \tag{30}$$

where $\boldsymbol{\eta}^{F*} = \mathsf{g}(\boldsymbol{y}, \Lambda, \boldsymbol{\eta}^L, t)$ stated before. Then, we define the Hamiltonian function for leader i as

$$\begin{aligned} H_i^L\big(\boldsymbol{y}, \Lambda, \boldsymbol{\eta}^L, \boldsymbol{\psi}_i, \boldsymbol{\phi}_i, t\big) = J_i\big(\eta_i^L, \mathsf{g}\big(\boldsymbol{y}, \Lambda, \boldsymbol{\eta}^L, t\big), t\big), \boldsymbol{\eta}^L_{\mathcal{L}\setminus i}\big) \\ + \boldsymbol{\psi}_i \dot{\boldsymbol{y}} + \sum_{m\in\mathcal{F}} \boldsymbol{\phi}_{mi} \dot{\boldsymbol{\lambda}}_m^T \end{aligned} \tag{31}$$

for $i \in \mathcal{L}$, where row vector $\boldsymbol{\psi}_i = [\psi_{ij}]_{j=1}^{2M}$ is the adjoint variables for the states $\boldsymbol{y}$, row vector $\boldsymbol{\phi}_{mi} = [\phi_{mij}]_{j=1}^{2M}$ is the adjoint variables for the adjoint variables $\boldsymbol{\lambda}_m$, and $\boldsymbol{\phi}_i = [\boldsymbol{\phi}_{mi}]_{m\in\mathcal{F}}$. Note that the last term $\boldsymbol{\phi}_{mi}\dot{\boldsymbol{\lambda}}_m^T$ is an inner product as $\dot{\boldsymbol{\lambda}}_m$ is a row vector, and $(\cdot)^T$ is the transpose operation.

We then have the optimality conditions (again applying Theorem 3)

$$\frac{\partial H_i^L\big(\boldsymbol{y}, \Lambda, \boldsymbol{\eta}^L, \boldsymbol{\psi}_i, \boldsymbol{\phi}_i, t\big)}{\partial \eta_i^L} = 0 \tag{32}$$

$$\dot{\boldsymbol{\psi}}_i = \rho\boldsymbol{\psi}_i - \frac{\partial H_i^L\big(\boldsymbol{y}, \Lambda, \boldsymbol{\eta}^L, \boldsymbol{\psi}_i, \boldsymbol{\phi}_i, t\big)}{\partial \boldsymbol{y}} \tag{33}$$

$$\dot{\boldsymbol{\phi}}_{mi} = \rho\boldsymbol{\phi}_{mi} - \frac{\partial H_i^L\big(\boldsymbol{y}, \Lambda, \boldsymbol{\eta}^L, \boldsymbol{\psi}_i, \boldsymbol{\phi}_i, t\big)}{\partial \boldsymbol{\phi}_{mi}} \tag{34}$$

for $i \in \mathcal{L}$ and $m \in \mathcal{F}$.

Different from the follower's game, there is one more transversality condition for an adjoint variable in the leader's problem, which depends on the costate variables in the follower's problem [53]. Let $\lambda_{mj} \in \Lambda$ where $j = 1, 2, \ldots, 2M$ and $m \in \mathcal{F}$ be a co-state variable in the follower's problem, and $\phi_{mij}(t) \in \boldsymbol{\phi}_{mi}$ be the costate variable of λ_{mj}. Then the costate variable $\lambda_{mj}(t)$ is called *uncontrollable* by the leader, if $\lambda_{mj}(0)$ is independent of the leader i's control path η_i, e.g., a function of time t only. Otherwise, it is said to be *controllable*. For those leaders' uncontrollable states, additional transversality conditions are needed, by setting $\phi_{mij}(0) = 0$.

Similarly, the concavity of the leader's Hamiltonian function H_i^L in (31) ensures η_i^{L*} can be uniquely expressed as a function of $\boldsymbol{y}, \Lambda, \boldsymbol{\eta}_{\mathcal{L}\setminus\{i\}}, \boldsymbol{\psi}_i, \boldsymbol{\phi}_i, t$ for all $i \in \mathcal{L}$. As such, after simplification, $\eta_i^{L*} = \mathsf{h}_i(\boldsymbol{y}, \Lambda, \boldsymbol{\psi}_i, \boldsymbol{\phi}_i, t)$, or the vector function $\boldsymbol{\eta}^{L*} = \mathsf{h}(\boldsymbol{y}, \Lambda, \Psi, \Phi, t)$, where $\Psi = [\boldsymbol{\psi}]_{i\in\mathcal{L}}$ and $\Phi = [\boldsymbol{\phi}_i]_{i\in\mathcal{L}}$. By backward induction, namely, substituting $\boldsymbol{\eta}^{L*} = \mathsf{h}(\boldsymbol{y}, \Lambda, \Psi, \Phi, t)$ into (28), (33), and (34) we can obtain the dynamics of the system states in (15), (29), (33), and (34) with only the states and time variable, i.e., $\boldsymbol{y}$, Λ, Ψ, Φ, and t. Together with the boundary conditions for the system states, a two point boundary value problem is defined, which can be solved numerically as stated earlier in Section V.

Algorithm 1: Implementation of Dynamic Hierarchical Framework

Input: VSPs' utility parameters, UAVs' parameters, and system parameters. Initialize $\boldsymbol{x}(0), \boldsymbol{z}(0)$.

Output: optimal control path $\boldsymbol{\eta}^*(t)$ and its associated system states $\boldsymbol{x}(t)$ and $\boldsymbol{z}(t)$

1: *Lower-level Evolutionary Game*
2: Compute $u_m(\boldsymbol{x}, \boldsymbol{\eta})$ for all $m \in \mathcal{M}$ and $\bar{u}$
3: **for** $m \in \mathcal{M}$ **do**
4: Derive the population dynamics given in Eq. (4)
5: **end for**
6: *Upper-level Differential Game*
7: **for** $m \in \mathcal{M}$ **do**
8: Obtain the objective functions $\mathfrak{J}_m$ in Eq. (5) and the Hamiltonian function H_m
9: Derive the dynamics for the co-states variables, namely Eq. (24) for simultaneous play and Eqs. (24), (33) and (34) for hierarchical play.
10: **end for**
11: Solve the boundary value problems to return $\boldsymbol{\eta}^*(t)$

The implementation is given in Algorithm 1. The complexity is as follows. Given that there are M players in the game, the population states $\boldsymbol{x}$ is of dimension $M-1$, and the DTs' value states $\boldsymbol{z}(t)$ is of dimension M. Thus, the overall number of system states is linear in M so are the co-states variables. Therefore, it is clear that steps 8 and 9 are of complexity $O(M)$ and step 4 has complexity $O(1)$. Therefore, the overall complexity is $O(M^2)$.

VII. Performance Evaluation

In this section, we examine and validate the theoretical findings presented in the previous section. First, we numerically demonstrate the existence, uniqueness, and stability of equilibrium obtained in the lower level evolutionary game (ESS). We then conduct sensitivity analyses by varying a series of system parameters, including the number M of VSPs, learning rate δ, decay rate θ_m, and discount rate ρ. Finally, we compare the results obtained by simultaneous differential game, Stackelberg differential game, and the static Stackelberg game. Parameters used in the simulation experiment are listed in Table II.

A. VSPs Are Simultaneous Decision Makers

1) Uniqueness and Existence of the ESS: We first consider the case that VSPs simultaneously determine their synchronization strategies. We first consider a representative case with two VSPs in the Metaverse, and the DT value decay rates for 2 VSPs are $\theta_1 = 0.05$ and $\theta_2 = 0.1$. Both VSPs have 80 DTs and the number of UAVs is 500. The learning rate is $\delta = 0.05$ and the discount rate is $\rho = 1$ for both VSPs. The initial values of the DTs are 40 for both VSPs. The time horizon $\mathcal{T} = [0, 300]$. The initial population states is given as $\boldsymbol{x}(0) = [0.5, 0.5]$ (i.e., without prior knowledge, the chance of

TABLE II
SIMULATION PARAMETERS

Parameters	Values
Total number of VSPs M	$[2, 4]$
UAV population size N	$[350, 500]$
Learning rate δ	$[0.01, 0.1]$
Discount rate ρ	$[0.05, 0.2]$
Number of DTs d_m	$[50, 120]$
Digital twins value decay rate θ_m	$[0.5, 1]$
Weight parameters $w_i, i = 1, 2, 3, 4$	$[0.001, 1]$
Data price α_m	0.1
Data contribution from each UAV each time b	$[0.1, 1]$ Mb
Average data size request rate k_m	$[0.1, 0.5]$ Mb
VSP's desired DT values v_m	60
Parameters for the affine mapping $g(\cdot)$, g_0, g_1	1

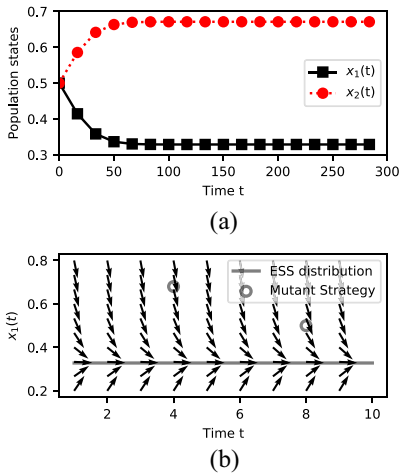

Fig. 3. Existence, uniqueness, and stability of the ESS in the lower level evolutionary game. (a) Evolution of UAV population states shows that the unique equilibrium in the lower level evolutionary game for two simultaneous decision-making VSPs. (b) Direction field of the replicator dynamics shows the evolutionary stability of the equilibrium in the lower level game.

selecting each VSP is the same among the UAV population at time 0).

To examine the existence and uniqueness of the lower level evolutionary game, we plot the trajectories of the population states over time in Fig. 3(a), which indicates the percentage of UAVs selecting each VSP over time. It can be seen that $x_2(t)$ increases steadily over time, while $x_1(t)$ decreases. After a few iterations, the population states $\boldsymbol{x}(t)$ reach an equilibrium state $\boldsymbol{x} = [0.33, 0.67]$. This numerically demonstrates the unique existence of the equilibrium in the lower level evolutionary game.

To further understand the reason why $x_2(t)$ increases over time, we plot the synchronization strategies of both VSPs in Fig. 4(a). We observe that on average VSP 2 adopts a higher synchronization rate than that of VSP 1. Because VSPs' synchronization strategy is positively correlated with the incentive pool offered to the UAVs, VSP 2 can issue more rewards to UAVs, and, therefore, UAVs that selected VSP 1 initially may switch their VSP selection to VSP 2 so as to enjoy higher payoffs, thereby increasing the value of $x_2(t)$ over time. However, as more UAVs select VSP 2, the average reward that a single device can receive decreases. Therefore, $x_2(t)$ stops increasing after some rounds of iterations and remains stable, i.e., reaches

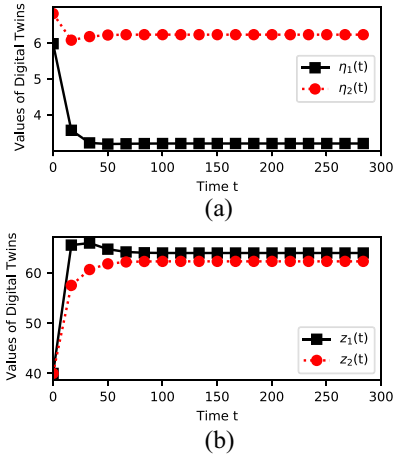

Fig. 4. Trajectories of controls and other system states in the simultaneous differential game with two VSPs. (a) Trajectories of synchronization intensity, chosen by each VSP. (b) Trajectories of the DTs' value states.

an equilibrium state, after which UAVs have no incentive to change their strategies.

2) Digital Twin Value States: After studying the evolution of the population states in the lower level evolutionary game $\boldsymbol{x}(t)$, we continue the analysis of the system state by plotting the evolution of DT value states, $\boldsymbol{z}(t)$, in Fig. 4(b). It can be seen that the DT values of both VSPs increase from their initial value of 40 toward the preferred threshold $v_m = 60$, after several iterations. In addition, we observe that the DT values of VSP 1 increase faster than those of VSP 2, in part due to the lower decay rate of VSP 1. The figure demonstrates the validity of our proposed solution, *IoT-assisted Metaverse synchronization*. In particular, to increase and preserve DT values at a certain preferred level, IoT can assist VSPs in collecting fresh data with respect to (w.r.t.) their real entities. The improved DT values result in a higher quality virtual business for VSPs as well as improving user experience.

3) Stability of Equilibrium in the Lower Level Evolutionary Game: Having demonstrated the ESS's unique existence in Section VII-A1, we now investigate the stability of the ESS, namely, if the mutant strategy in the UAV population can evolve toward the ESS, given a small perturbation around the equilibrium point. We only examine $x_1(t)$ as $x_2(t) = 1 - x_1(t)$. We vary $x_1(0) \in [0.2, 0.8]$ in step size of 0.067 while fixing the digital value states $\boldsymbol{z}(t)$, the same as their equilibrium in the last section (Section VII-A2). Fig. 3(b) shows the evolution direction of $x_1(t)$ over time. Clearly, the population states converge to the ESS ($x_1 = 0.33$) from any initial strategy distribution over the UAV population. In addition, mutant strategies could be eliminated by the adaptive process of VSP selection, which demonstrates the robustness and stability of the ESS in the lower level game.

B. Sensitivity Analysis

We now study the sensitivity of the results to changes in system parameter values, including the number of UAVs M, learning rate δ, and decay parameter θ_m.

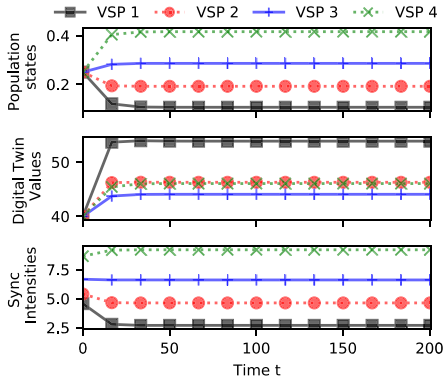

Fig. 5. Trajectories of population states $\boldsymbol{x}(t)$, DT values $\boldsymbol{z}(t)$, and synchronization intensities $\boldsymbol{\eta}(t)$ for the simultaneous differential game with $M = 4$, exhibiting similar patterns as those of previous experiments with $M = 2$.

1) Varying M, the Number of VSPs in the Metaverse: We first consider a case with a larger value $M = 4$. The parameters for VSPs 1 and 2 are identical to those in Section VII.The parameters of the additional two VSPs are $d_3 = 80$, $d_4 = 80$, $\theta_3 = 0.15$, and $\theta_4 = 0.2$. The initial population states is $\boldsymbol{x}(0) = [0.25, 0.25, 0.25, 0.25]$. The initial DT values are $\boldsymbol{z}(0) = [40, 40, 40, 40]$.

Fig. 5 shows the trajectories of the population states $\boldsymbol{x}(t)$, synchronization intensities $\boldsymbol{\eta}(t)$, as well as the their DT values $\boldsymbol{z}(t)$. In general, we observe a similar pattern to the case of $M = 2$, namely, all trajectories converge in the long run. This means the dynamic interactions between the VSPs and UAVs become stable after several rounds of iterations. In particular, for $\boldsymbol{x}$, we observe that $x_4(t)$ increases over time, as VSP 4 increases its synchronization intensity in response to the higher decay rate of its DTs. As a result, higher incentives (as positively correlated with the synchronization intensity) can attract more UAVs to aid the collection of synchronization data for VSP 4. However, as shown in the second subfigure of Fig. 5, DTs from VSP 1 are of the highest values over time, even though its UAV selection is the lowest. The reason is that the decay rate of VSP 1 is the lowest. With the minimal provision of synchronization data, the values of its DTs can still be maintained. In contrast, though the selection of VSP 4 is the highest among the UAV population, it is still not enough to improve the DT values of VSP 4 to reach the threshold, 60.

2) Varying δ, Learning Rate in the Evolutionary Dynamics: The effect of the learning rate δ on the simultaneous differential game of the four VSPs can be seen in Fig. 6. The experiment parameters are the same as presented in Section VII-B1, except for $\delta \in \{0.01, 0.02, 0.1\}$. Fig. 6(a) shows the trajectories of the population states $x_1(t)$, $x_2(t)$, and $x_3(t)$ under different values of δ. Clearly, $\delta = 0.1$ gives the fastest convergence speed of the population states in the evolutionary game, whereas $\delta = 0.01$ gives the slowest speed. This can be explained by the fact that the learning rate reflects the strategy adaptation frequency, e.g., the percentage of UAVs adjusting their VSP selection at each time instant. Consequently, learning rates control how quickly strategies converge in the lower level evolutionary game.

Fig. 6(b) shows the trajectories synchronization intensities $\boldsymbol{\eta}(t)$ of four VSPs under various values of learning rate in

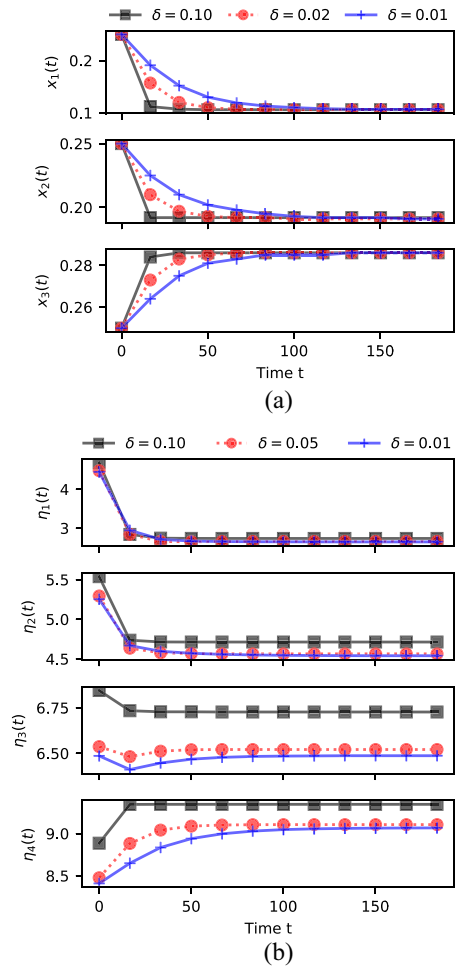

Fig. 6. Sensitivity analysis of learning rate δ. (a) Population states. (b) Sync intensities.

the lower level game. First, we observe that there is a stable strategy for all the VSPs after a few iterations for any value of δ. In addition, similar to the findings in Fig. 6(a), we can also observe that the lower the value of δ, the longer it takes to achieve a stable control strategy. However, unlike $\boldsymbol{x}(t)$ in Fig. 6(a) that it always converge to the same equilibrium state under various δ, we observe that the equilibrium synchronization intensities are at different values under the different values of δ, especially for VSPs with higher decay rates, such as VSPs 3 and 4 in the experiment. The reason is that players (VSPs) in the upper level game make decisions (synchronization intensity) based on discounted accumulative payoffs, and that recent payoffs carry greater weight on cumulative payoffs. Note that an even selection of VSPs in the UAV population does not favor VSPs 3 and 4 because they may require more UAVs to assist the task due to higher decay rates. Therefore, a small learning rate in the lower level game can make VSPs 3 and 4 stay in the unfavored position for a longer time and decrease the overall discounted payoff. Subsequently, VSPs may decide to reduce their synchronization intensity in response to this situation.

In contrast, selections of VSPs by UAVs modeled by the replicator dynamics in evolutionary games, are myopic. UAVs only target payoffs in the infinitesimal vicinity of the present

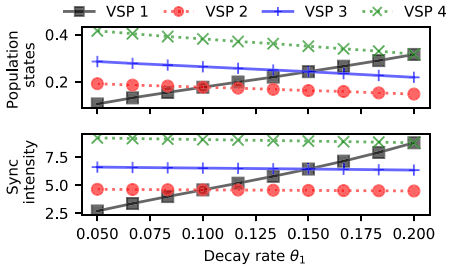

Fig. 7. Sensitivity analysis of DT value decay rate θ_1.

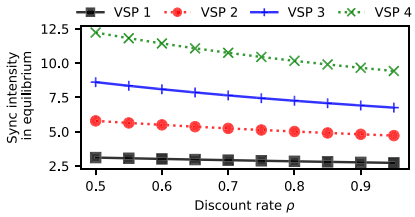

Fig. 8. Sensitivity analysis of time discount rate ρ.

time without discounting those future payoffs or referring to the long-term memory. With such a myopic nature, population states can always reach the same set of equilibrium states given the varying learning rates.

3) Varying θ_m, the Decay Rate of VSP: The impact of the decay rate θ on the lower level game (UAVs' VSP selection distribution) and the upper level game (VSPs' synchronization intensity) is shown in Fig. 7. While keeping all the parameters the same as in the previous experiment, we set the learning rate δ as 0.05 and vary the decay rate for VSP 1, i.e., $\delta_1 \in [0.05, 0.2]$ in step size of 0.0167. We plot populations states $\boldsymbol{x}$ in equilibrium and synchronization intensity $\boldsymbol{\eta}$ in equilibrium for all VSPs. We observe that the value of $\eta_1(t)$ increases as the decay rate of VSP 1 increases, whereas $\eta_i(t), i = 2, 3, 4$ decrease. The reason is that a higher decay rate of DTs indicates that VSP 1 requires more synchronization data to maintain its DT status, and, therefore, VSP 1 increases its synchronization intensity in response. Faced with a higher incentive offered by VSP 1, more UAVs adjust their strategies to work for VSP 1, thereby increasing $x_1(t)$. However, subject to a limited number of UAVs assisting the Metaverse, data provisions to other VSPs are affected. Consequently, we observe a decrease in synchronization intensity for the remaining VSPs as well as fewer UAV selections. The result demonstrates the dynamic interactions between the two levels of the game, i.e., between the VSPs and UAVs.

4) Varying ρ, the Discount Rate: Fig. 8 shows the effect of VSPs' discount rate ρ on the synchronization intensity $\boldsymbol{\eta}$ in equilibrium. We keep the experiment parameters the same as in the last experiment and set the value of δ_1 to 0.05. Then, we vary $\rho \in [0.5, 1]$ in step size of 0.05. We observe that the synchronization intensities for all VSPs decrease as the value of the discount factor increases. The reason is that the higher value of ρ, the lower the value of $e^{-\rho t}$ given a fixed t, thereby having a greater discounting effect on the future instantaneous utility at the time t. Therefore, $\mathfrak{J}_m, m = 1, 2, 3, 4$, the discounted cumulative payoffs, for all VSPs are smaller. In response, all VSPs lower their synchronization intensity.

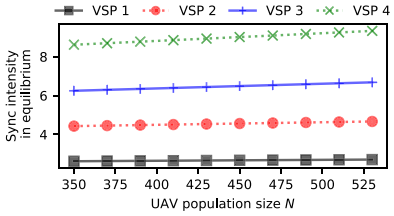

Fig. 9. Sensitivity analysis of UAVs population size N.

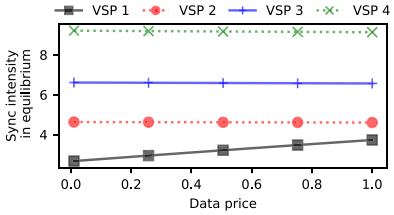

Fig. 10. Sensitivity analysis of data price α_1.

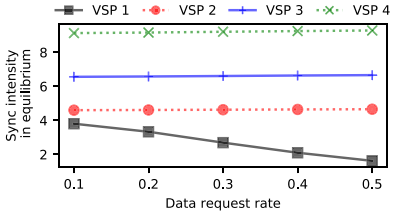

Fig. 11. Sensitivity analysis of data request rate k_1.

5) Varying N, the Size of UAV Population: Fig. 9 shows the effect of UAVs population size n on the synchronization intensity $\boldsymbol{\eta}$ in equilibrium. We keep the experiment parameters the same as in the last experiment and set the value of N from 350 to 550 in step size of 20. We observe that the synchronization intensities for all VSPs increase as N increases. Because the higher value of N is, the more data that can be supplied by the IoT group, thereby allowing the VSPs to have a higher synchronization intensity. Among the four VSPs, the increase for VSP 4 is the most significant because its DTs have higher decay rates and, therefore, require higher synchronization data supply.

6) Varying α_m, the Data Price: Fig. 10 shows the effect of data price α_m on the synchronization intensity $\boldsymbol{\eta}$ in equilibrium in the upper level game. We keep the experiment parameters the same as in the last experiment and vary the value of α_1 from 0.01 to 1. We observe that the synchronization intensities for VSP 1 increase as the value of the α_1 increases. Because the higher value of α_1 indicates more accumulated payoffs can be obtained by VSP 1, this allows VSP 1 to afford a higher synchronization intensity. In contrast, the synchronization intensities for the remaining VSPs declined slightly. The reason is that more UAVs choose VSP 1 and with a lower synchronized data supply, the synchronization intensities for the remaining VSPs drop.

7) Varying k_m, the Data Request Rate: Fig. 11 shows the effect of data request rate by DTs on the synchronization intensity $\boldsymbol{\eta}$ in equilibrium for the upper level game. We keep the experiment parameter values the same as in the last experiment and vary the value of k_1 from 0.1 to 0.5. We

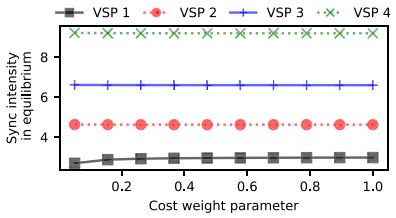

Fig. 12. Sensitivity analysis of cost weight parameter w_1^3.

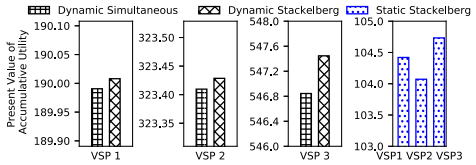

Fig. 13. Comparison of the accumulative payoffs discounted at the present time for Stackelberg differential game, simultaneous differential game, and static Stackelberg game (baseline).

observe that the synchronization rate for VSP 1 decreases as the value of k_1 increases. The higher value of k_1 implies that more synchronization data are needed for one-time synchronization. In order to meet the demand for DTs based on the data supplied from UAVs, the VSPs choose to decrease the synchronization intensity such that demand and supply can be matched.

8) Varying w_m^3, the Cost Weight Parameter in the Objective Functional: Fig. 12 shows the effect of the cost weight parameter w_1^3 on the synchronization intensity $\boldsymbol{\eta}$ in equilibrium in the upper level game. w_1^3 is the weight parameter for the penalty term (i.e., cost to the VSPs) when the DTs' values are not meeting the threshold. We keep the experiment parameter values the same as in the last experiment and vary the cost weight parameter value of w_1^3 from 0.01 to 0.03. We observe that the synchronization rate for VSP 1 increases as the value of w_1^3 increases. The higher value of w_1^3 implies that more costs are incurred to VSP 1 if the DTs' values are far away from the expected values. In response, VSP 1 increases its synchronization intensity. Moreover, when the cost weight parameter is sufficiently large, the synchronization intensity at the equilibrium becomes unchanged. The reason is that the cost incurred by low-valued DTs dominates the VSP 1's objective functional and, therefore, VSP 1's equilibrium strategy becomes similar when the weight term is large.

C. Comparison With the Hierarchical Play

We conducted an experiment to compare three cases: 1) simultaneous moves VSPs, i.e., a simultaneous differential game; 2) hierarchical moves VSPs (i.e., the Stackelberg differential game, as presented in Section VI); and 3) a static Stackelberg game with an evolutionary game, as a benchmark. In the static Stackelberg game, there is no dynamic interaction between VSPs and UAVs: VSPs perform do a one-step optimization at the very beginning, and then UAVs populations evolve with the static synchronization intensity. In other words, in the static Stackelberg game, $\eta_m(t) = C_m \quad \forall t$, where C_m is some constant that optimizes VSP m's strategy. The steps to obtain a solution for a static Stackelberg game can be found in [55]. For illustration, we consider the case of one leader and two followers in the Stackelberg differential game and three simultaneous VSPs in the simultaneous differential game. As for the experiment setting, we consider VSPs 1 to 3 from the previous experiment and allow VSP 3 to be the leader. Additionally, we set $\delta = 0.02$ and $\rho = 1$.

As shown in Fig. 13, both the Stackelberg differential game and simultaneous differential game provide higher discounted cumulative payoffs than the static Stackelberg game. The reason is that both the Stackelberg differential game and simultaneous differential game capture the dynamic interactions between VSPs and UAVs and, thus, optimize the synchronization intensity control over time. It can also be observed that the Stackelberg differential game yields slightly higher discounted cumulative payoffs than the simultaneous differential game, especially for the leader. The reason is that the leader's decision can affect the followers' decisions and, thus, the synchronization intensity control obtained by VSP 3 (leader) under the Stackelberg differential game can help improve the overall discounted utilities.

VIII. Conclusion

In this article, we proposed a dynamic hierarchical framework to address the problem of DT synchronization for the VSPs in the Metaverse with assistance from UAVs. In particular, we proposed a temporal value decay dynamics to measure the DT values and how they are affected by the VSPs synchronization strategy. In addition, a group of UAVs can assist VSPs to collect the most up-to-date status data of the physical counterparts to the DTs. Then, we adopted an evolutionary game to model the dynamic VSP selection behaviors for the population of UAVs. Open-loop Nash solutions were used to determine the optimal controls for the VSPs in the upper level after formulating the upper level problem as a differential game. To make the solution more realistic, we also considered the case where a group of VSPs can be the first movers in the market, and formulated it as a Stackelberg differential game. Experiments and proofs showed that the equilibrium point of the lower level game exists and is evolutionarily stable. In addition, the experiments demonstrated that dynamical games (both simultaneous differential game and Stackelberg differential game) outperform the static Stackelberg game. The equilibrium adaptation for different system parameters was also investigated. The extension to interoperability among VSPs will be considered in future work.

Appendix A
Equilibrium Uniqueness and Existence

Proof: Let the right-hand side of (4) denote by $f_m(\boldsymbol{x}, \boldsymbol{\eta})$. For fixed control path $\boldsymbol{\eta}(t)$, let $\tilde{f}_m(\boldsymbol{x}, t) := f_m(\boldsymbol{x}, \boldsymbol{\eta})$. Then, the differential equation (4) reduces to the ordinary differential equation

$$\dot{x}_m(t) = \tilde{f}_m(\boldsymbol{x}, t) \quad \forall m \in \mathcal{M}. \tag{35}$$

First, $\tilde{f}_m$ is continuous when $\boldsymbol{\eta}(t)$ is continuous. Next, for a fixed time t and given control sequence $\boldsymbol{\eta}(t)$, the utility $u_m(t)$ is bounded, achieving maximum value when $x_m = 1/d_m$ and the minimum value when $x_m = 1$ for $x_m > 0$. If $x_m = 0$, $u_m \equiv 0$ and is bounded as well. Therefore, the partial derivative of u_m w.r.t x_m, $([\partial u_m]/[\partial x_m])$, is bounded and, thus, $([\partial u_m]/[\partial x_q]) = 0$ for $q \neq m$. Therefore, $([\partial \bar{u}]/[\partial x_m]) = u_m + x_m([\partial u_m]/x_m)$ is bounded as well. Next, we can show that the partial derivatives of $\tilde{f}_m$ w.r.t. x_q for $q \neq m$ is bounded, since $([\partial \tilde{f}_m]/[\partial x_q]) = -\delta x_m[u_q + x_q([\partial u_q]/[\partial x_q])]$ and partial derivatives of $\tilde{f}_m$ w.r.t. x_m is bounded given that $([\partial \tilde{f}_m]/[\partial x_q]) = \delta(u_m - \bar{u}) + \delta x_m[([\partial u_m]/[\partial x_m]) - ([\partial \bar{u}]/[\partial x_m])]$. Thus, $\tilde{\boldsymbol{f}}$ is bounded for all $(\boldsymbol{x}, t) \in \Delta \times \mathbb{R}$, i.e., the Cartesian product of the state space and the 1-D real space. Therefore, by the mean value theorem, it can be proved that $|\tilde{f}_m(\boldsymbol{x}, t) - \tilde{f}_m(\boldsymbol{y}, t)|/|\boldsymbol{x} - \boldsymbol{y}|$ is bounded for all $t \in \mathbb{R}$, which implies that $\tilde{f}_m(\boldsymbol{x}, t)$ satisfies the global Lipschitz condition [56] and, consequently, a unique solution to the dynamical system exists globally. ■

APPENDIX B
EQUILIBRIUM STABILITY

Proof: We adopt the Lyapunov direct method [19] for the proof, by showing that the time derivative of the Lyapunov function is strictly negative. Let $\boldsymbol{x}^* = [x_m]_{m \in \mathcal{M}}$ be the interior stationary points and let the error function denote by $e_m(t) \coloneqq x_m^*(t) - x_m(t)$. In this regard, a Lyapunov function $V_m : \mathcal{T} \to \mathbb{R}_+$ can be defined by $V_m = e_m^2(t)/2$. Its time derivative $\dot{V}_m$ can be derived as follows:

$$\dot{V}_m = -e_m \delta x_m (u_m - \bar{u}). \tag{36}$$

When $u_m > \bar{u}$, the population ratio x_m increases, and, therefore, $e_m(t) > 0$. As $x_e \neq 0$, we have $\dot{V}_e < 0$. When $u_m < \bar{u}$, the population ratio x_m decreases, and, therefore, $x_m(t) < 0$, which also implies $\dot{V}_e < 0$. Therefore, the interior stationary point is asymptotically stable, based on the Lyapunov stability theory. ■

REFERENCES

[1] "Watch Blockeley, UC Berkeley's online minecraft commencement." May 2020. Accessed: Mar. 13, 2022. [Online]. Available: https://news.berkeley.edu/2020/05/16/watch-blockeley-uc-berkeleys-online-minecraft-commencement/

[2] "Fortnite's Marshmello concert was the game's biggest event ever—The verge." Accessed: Mar. 13, 2022. [Online]. Available: https://www.theverge.com/2019/2/21/18234980/fortnite-marshmello-concert-viewer-numbers

[3] L.-H. Lee *et al.*, "All one needs to know about metaverse: A complete survey on technological singularity, virtual ecosystem, and research agenda," Oct. 2021, *arXiv:2110.05352*.

[4] J. D. N. Dionisio, W. G. Burns, III, and R. Gilbert, "3D virtual worlds and the metaverse: Current status and future possibilities," *ACM Comput. Surv.*, vol. 45, no. 3, pp. 1–38, 2013.

[5] J. Shurvell. "Take a virtual African Safari in 2020 in real-time from your sofa." Accessed: Mar. 16, 2022. [Online]. Available: https://www.forbes.com/sites/joanneshurvell/2020/05/15/take-a-virtual-african-safari-in-2020-in-real-time-from-your-sofa/

[6] "Virtual theme park rides you can experience from home—Tips—The Jakarta post." Accessed: Mar. 16, 2022. [Online]. Available: https://www.thejakartapost.com/travel/2020/03/31/virtual-theme-park-rides-you-can-experience-from-home.html

[7] R. Schroeder, "Social interaction in virtual environments: Key issues, common themes, and a framework for research," in *The Social Life of Avatars*. London, U.K.: Springer, 2002, pp. 1–18.

[8] J. Radoff. "Web3, interoperability and the metaverse." Nov. 2021. Accessed: Mar. 16, 2022. [Online]. Available: https://medium.com/building-the-metaverse/web3-interoperability-and-the-metaverse-5b252dc39da

[9] E. Gadalla, K. Keeling, and I. Abosag, "Metaverse-retail service quality: A future framework for retail service quality in the 3D Internet," *J. Market. Manag.*, vol. 29, nos. 13–14, pp. 1493–1517, Oct. 2013.

[10] A. O. Kwok and S. G. Koh, "COVID-19 and extended reality (XR)," *Current Issues Tour.*, vol. 24, no. 14, pp. 1935–1940, 2021.

[11] J. E. M. Díaz, C. A. D. Saldaña, and C. A. R. Avila, "Virtual world as a resource for hybrid education," *Int. J. Emerg. Technol. Learn.*, vol. 15, no. 15, pp. 94–109, 2020.

[12] H. Duan, J. Li, S. Fan, Z. Lin, X. Wu, and W. Cai, "Metaverse for social good: A university campus prototype," in *Proc. ACM Multimedia*, 2021, pp. 153–161.

[13] O. Michel. "Virtual travel experiences to enjoy now." Accessed: Nov. 16, 2021. [Online]. Available: https://www.boatinternational.com/destinations/virtual-travel-tours-trips-vr-experiences--43207

[14] L. U. Khan, W. Saad, D. Niyato, Z. Han, and C. S. Hong, "Digital-twin-enabled 6G: Vision, architectural trends, and future directions," Nov. 2021, *arXiv:2102.12169*.

[15] S. M. Taheri, K. Matsushita, and M. Sasaki, "Virtual reality driving simulation for measuring driver behavior and characteristics," *J. Transp. Technol.*, vol. 7, no. 2, pp. 123–132, 2017.

[16] K. Bhatt, A. Pourmand, and N. Sikka, "Targeted applications of unmanned aerial vehicles (drones) in telemedicine," *Telemed. J. E Health*, vol. 24, no. 11, pp. 833–838, Nov. 2018.

[17] A. Sanjab, W. Saad, and T. Başar, "Prospect theory for enhanced cyber-physical security of drone delivery systems: A network interdiction game," in *Proc. ICC*, 2017, pp. 1–6.

[18] C. Kam, S. Kompella, G. D. Nguyen, J. E. Wieselthier, and A. Ephremides, "Information freshness and popularity in mobile caching," in *Proc. ISIT*, 2017, pp. 136–140.

[19] J. W. Weibull, *Evolutionary Game Theory*. Cambridge, MA, USA: MIT Press, 1997.

[20] D. Brown, *Big Tech Wants to Build the 'Metaverse.' What on Earth Does That Mean?* Washington Post, Washington, DC, USA, Aug. 2021.

[21] D. Volk, "Co-creative game development in a participatory metaverse," in *Proc. ACM PDC*, 2008, pp. 262–265.

[22] C. T. Nguyen, D. T. Hoang, D. N. Nguyen, and E. Dutkiewicz, "MetaChain: A novel blockchain-based framework for metaverse applications," Dec. 2021, *arXiv:2201.00759*.

[23] Y. Jiang, J. Kang, D. Niyato, X. Ge, Z. Xiong, and C. Miao, "Reliable coded distributed computing for metaverse services: Coalition formation and incentive mechanism design," Nov. 2021, *arXiv:2111.10548*.

[24] W. Y. B. Lim *et al.*, "Realizing the metaverse with edge intelligence: A match made in heaven," Jan. 2022, *arXiv:2201.01634*.

[25] Y. Han, D. Niyato, C. Leung, C. Miao, and D. I. Kim, "A dynamic resource allocation framework for synchronizing metaverse with IoT service and data," Oct. 2021, *arXiv:2111.00431*.

[26] J. Radoff. "The metaverse value-chain." Jun. 2021. Accessed: Sep. 8, 2021. [Online]. Available: https://medium.com/building-the-metaverse/the-metaverse-value-chain-afcf9e09e3a7

[27] Y. Lu, X. Huang, K. Zhang, S. Maharjan, and Y. Zhang, "Communication-efficient federated learning and permissioned blockchain for digital twin edge networks," *IEEE Internet Things J.*, vol. 8, no. 4, pp. 2276–2288, Feb. 2021.

[28] I. Yaqoob, K. Salah, M. Uddin, R. Jayaraman, M. Omar, and M. Imran, "Blockchain for digital twins: Recent advances and future research challenges," *IEEE Netw.*, vol. 34, no. 5, pp. 290–298, Sep./Oct. 2020.

[29] S. Mangiante, G. Klas, A. Navon, Z. GuanHua, J. Ran, and M. D. Silva, "VR is on the edge: How to deliver 360° videos in mobile networks," in *Proc. ACM SIGCOMM*, 2017, pp. 30–35.

[30] B. Marr. "What is extended reality technology? A simple explanation for anyone." Accessed: Nov. 14, 2021. [Online]. Available: https://www.forbes.com/sites/bernardmarr/2019/08/12/what-is-extended-reality-technology-a-simple-explanation-for-anyone/

[31] A. El Saddik, "Digital twins: The convergence of multimedia technologies," *IEEE MultiMedia*, vol. 25, no. 2, pp. 87–92, Apr.–Jun. 2018.

[32] D. M. Müller. "NFT's next step: Cyber-physical assets." Jan. 2022. Accessed: Feb. 21, 2022. [Online]. Available: https://medium.com/deep-tech-innovation/nfts-next-step-cyber-physical-assets-e32046c46197

[33] C. Nunley. "People in the Philippines are earning cryptocurrency during the pandemic by playing a video game." May 2021. Accessed: Sep. 14, 2021. [Online]. Available: https://www.cnbc.com/2021/05/14/people-in-philippines-earn-cryptocurrency-playing-nft-video-game-axie-infinity.html

[34] Y. Chen and C. Bellavitis, "Blockchain disruption and decentralized finance: The rise of decentralized business models," *J. Bus. Venturing Insights*, vol. 13, Jun. 2020, Art. no. e00151.

[35] A. Moneta, "Architecture, heritage and metaverse: New approaches and methods for the digital built environment," *Traditional Dwellings Settlements Rev.*, vol. 32, no. 2, p. 1, 2020.

[36] M. Grieves, "Digital twin: Manufacturing excellence through virtual factory replication," Melbourne, FL, USA, Florida Inst. Technol., White Paper, vol. 1, pp. 1–7, 2014.

[37] E. H. Glaessgen and D. S. Stargel, "The digital twin paradigm for future NASA and U.S. air force vehicles," in *Proc. 53rd AIAA/ASME/ASCE/AHS/ASC Struct. Struct. Dyn.*, 2012, pp. 1–14.

[38] A. Fuller, Z. Fan, C. Day, and C. Barlow, "Digital twin: Enabling technologies, challenges and open research," *IEEE Access*, vol. 8, pp. 108952–108971, 2020.

[39] F. Tao, H. Zhang, A. Liu, and A. Y. C. Nee, "Digital twin in industry: State-of-the-art," *IEEE Trans. Ind. Informat.*, vol. 15, no. 4, pp. 2405–2415, Apr. 2019.

[40] T. Gabor, L. Belzner, M. Kiermeier, M. T. Beck, and A. Neitz, "A simulation-based architecture for smart cyber-physical systems," in *Proc. IEEE Int. Conf. Autom. Comput.*, 2016, pp. 374–379.

[41] S. Weyer, T. Meyer, M. Ohmer, D. Gorecky, and D. Zühlke, "Future modeling and simulation of CPS-based factories: An example from the automotive industry," *IFAC-PapersOnLine*, vol. 49, no. 31, pp. 97–102, Jan. 2016.

[42] "Cyber-physical systems (CPS) U.S. national science foundation." Accessed: Mar. 3, 2022. [Online]. Available: https://www.nsf.gov/pubs/2010/nsf10515/nsf10515.htm

[43] "AR and VR technologies are revolutionizing metaverse. Here's how?" Jan. 2022. Accessed: Mar. 5, 2022. [Online]. Available: https://www.analyticsinsight.net/ar-and-vr-technologies-are-revolutionizing-metaverse-heres-how/

[44] W. Wang, X. Li, L. Xie, H. Lv, and Z. Lv, "Unmanned aircraft system airspace structure and safety measures based on spatial digital twins," *IEEE Trans. Intell. Transp. Syst.*, vol. 23, no. 3, pp. 2809–2818, Mar. 2022.

[45] *Linear Utility*, Wikipedia, San Francisco, CA, USA, May 2021.

[46] J.-Y. Jaffray, "Linear utility theory for belief functions," *Oper. Res. Lett.*, vol. 8, no. 2, pp. 107–112, Apr. 1989.

[47] R. Shakeri *et al.*, "Design challenges of multi-UAV systems in cyber-physical applications: A comprehensive survey and future directions," *IEEE Commun. Surveys Tuts.*, vol. 21, no. 4, pp. 3340–3385, 4th Quart., 2019.

[48] W. Y. B. Lim *et al.*, "Towards federated learning in UAV-enabled Internet of vehicles: A multi-dimensional contract-matching approach," *IEEE Trans. Intell. Transp. Syst.*, vol. 22, no. 8, pp. 5140–5154, Aug. 2021.

[49] Y. Han, D. Niyato, C. Leung, and D. I. Kim, "Opportunistic coded distributed computing: An evolutionary game approach," in *Proc. IEEE IWCMC*, 2021, pp. 1430–1435.

[50] D. Niyato and E. Hossain, "Dynamics of network selection in heterogeneous wireless networks: An evolutionary game approach," *IEEE Trans. Veh. Technol.*, vol. 58, no. 4, pp. 2008–2017, May 2009.

[51] K. Zhu, E. Hossain, and D. Niyato, "Pricing, spectrum sharing, and service selection in two-tier small cell networks: A hierarchical dynamic game approach," *IEEE Trans. Mobile Comput.*, vol. 13, no. 8, pp. 1843–1856, Aug. 2014.

[52] X. Liu, H. Song, and A. Liu, "Intelligent UAVs trajectory optimization from space-time for data collection in social networks," *IEEE Trans. Netw. Sci. Eng.*, vol. 8, no. 2, pp. 853–864, Apr.–Jun. 2021.

[53] E. J. Dockner, S. Jorgensen, N. V. Long, and G. Sorger, *Differential Games in Economics and Management Science*. Cambridge, U.K.: Cambridge Univ. Press, 2000.

[54] S. P. Sethi, *Optimal Control Theory: Applications to Management Science and Economics*. Cham, Switzerland: Springer Int., 2019.

[55] M. Simaan and J. B. Cruz, "On the Stackelberg strategy in nonzero-sum games," *J. Optim. Theory Appl.*, vol. 11, no. 5, pp. 533–555, 1973.

[56] J. Engwerda, *LQ Dynamic Optimization and Differential Games*. Chichester, U.K.: Wiley, 2005.

Yue Han received the B.Sc. degree (First Class Hons.) in mathematical sciences from Nanyang Technological University, Singapore, in 2015, where she is currently pursuing the Ph.D. degree with the Alibaba Group and the Alibaba-NTU Joint Research Institute.

She was previously a Data Scientist with NTUC Enterprise, Singapore, from 2017 to 2019, and a Data Science Consulting Analyst with Accenture, Singapore, from 2015 to 2017. Her research interests include game theory and its applications in Internet of Things, edge computing, and Metaverse.

Dusit Niyato (Fellow, IEEE) received the B.Eng. degree from the King Mongkuts Institute of Technology Ladkrabang, Bangkok, Thailand, in 1999, and the Ph.D. degree in electrical and computer engineering from the University of Manitoba, Winnipeg, MB, Canada, in 2008.

He is currently a Professor with the School of Computer Science and Engineering, Nanyang Technological University, Singapore. His research interests are in the areas of Internet of Things, machine learning, and incentive mechanism design.

Cyril Leung (Life Member, IEEE) received the B.Sc. degree (First Class Hons.) from Imperial College, University of London, London, U.K., in 1973, and the M.S. and Ph.D. degrees in electrical engineering from Stanford University, Stanford, CA, USA, in 1974 and 1976, respectively.

He has been an Assistant Professor with the Department of Electrical Engineering and Computer Science, Massachusetts Institute of Technology, Cambridge, MA, USA, and the Department of Systems Engineering and Computing Science, Carleton University, Ottawa, ON, Canada. He served as an Associate Dean for Research and Graduate Studies with the Faculty of Applied Science, The University of British Columbia, Vancouver, BC, Canada, from 2008 to 2011, where he is currently a Professor with the Department of Electrical and Computer Engineering, and holds the PMC-Sierra Professorship in Networking and Communications. His research interests include wireless communication systems, network security, and technologies to support ageless aging for the elderly.

Dr. Leung is a member of the Association of Professional Engineers and Geoscientists of British Columbia, Canada, and a Fellow of the Engineering Institute of Canada.

Dong In Kim (Fellow, IEEE) received the Ph.D. degree in electrical engineering from the University of Southern California, Los Angeles, CA, USA, in 1990.

He was a tenured Professor with the School of Engineering Science, Simon Fraser University, Burnaby, BC, Canada. Since 2007, he has been an SKKU-Fellowship Professor with the College of Information and Communication Engineering, Sungkyunkwan University, Suwon, South Korea.

Dr. Kim has been the first recipient of the NRF of Korea Engineering Research Center in Wireless Communications for RF Energy Harvesting since 2014. He has been listed as a 2020 Highly Cited Researcher by Clarivate Analytics. He was selected the 2019 recipient of the IEEE Communications Society Joseph LoCicero Award for Exemplary Service to Publications. He is the General Chair for IEEE ICC 2022 in Seoul. He served as an Editor and an Editor-at-Large of Wireless Communications I for the IEEE TRANSACTIONS ON COMMUNICATIONS from 2001 to 2020. He also served as an Editor and a Founding Area Editor of Cross-Layer Design and Optimization for the IEEE TRANSACTIONS ON WIRELESS COMMUNICATIONS from 2002 to 2011. He served as the Co-Editor-in-Chief for the IEEE/KICS JOURNAL OF COMMUNICATIONS AND NETWORKS from 2008 to 2011. He served as the Founding Editor-in-Chief for the IEEE WIRELESS COMMUNICATIONS LETTERS from 2012 to 2015. He is a Fellow of the Korean Academy of Science and Technology and a Member of the National Academy of Engineering of Korea.

Kun Zhu (Member, IEEE) received the Ph.D. degree from the School of Computer Engineering, Nanyang Technological University, Singapore, in 2012.

He was a Research Fellow with the Wireless Communications Networks and Services Research Group, University of Manitoba, Winnipeg, MB, Canada, from 2012 to 2015. He is currently a Professor with the College of Computer Science and Technology, Nanjing University of Aeronautics and Astronautics, Nanjing, China. He is also a Jiangsu Specially Appointed Professor. He has published more than 80 technical papers and has served as TPC for several conferences. His research interests include resource allocation in wireless networks, autonomous driving networks, and edge intelligence.

Prof. Zhu won several research awards, including the IEEE WCNC 2019 Best Paper Awards and the ACM China Rising Star Chapter Award.

Shaohan Feng received the B.S. degree from the School of Mathematics and Systems Science, Beihang University, Beijing, China, in 2014, the M.S. degree from the School of Mathematical Sciences, Zhejiang University, Hangzhou, China, in 2016, and the Ph.D. degree from the School of Computer Science and Engineering, Nanyang Technological University, Singapore, in 2020.

His current research interests include risk management and resource allocation in cloud computing and communication networks.

Xuemin (Sherman) Shen (Fellow, IEEE) received the Ph.D. degree in electrical engineering from Rutgers University, New Brunswick, NJ, USA, in 1990.

He is a University Professor with the Department of Electrical and Computer Engineering, University of Waterloo, Waterloo, ON, Canada. His research focuses on network resource management, wireless network security, Internet of Things, 5G and beyond, and vehicular networks.

Dr. Shen received the Canadian Award for Telecommunications Research from the Canadian Society of Information Theory in 2021, the R.A. Fessenden Award in 2019 from IEEE, Canada, the Award of Merit from the Federation of Chinese Canadian Professionals (Ontario) in 2019, the James Evans Avant Garde Award in 2018 from the IEEE Vehicular Technology Society, the Joseph LoCicero Award in 2015 and the Education Award in 2017 from the IEEE Communications Society (ComSoc), and the Technical Recognition Award from Wireless Communications Technical Committee in 2019 and AHSN Technical Committee in 2013. He has also received the Excellent Graduate Supervision Award in 2006 from the University of Waterloo and the Premier's Research Excellence Award in 2003 from the Province of Ontario, Canada. He served as the Technical Program Committee Chair/Co-Chair for IEEE Globecom'16, IEEE Infocom'14, IEEE VTC'10 Fall, and IEEE Globecom'07, and the Chair for the IEEE ComSoc Technical Committee on Wireless Communications. He is the President of the IEEE ComSoc. He was the Vice President for Technical and Educational Activities and Publications, a Member-at-Large on the Board of Governors, the Chair of the Distinguished Lecturer Selection Committee, and a member of IEEE Fellow Selection Committee of the ComSoc. He served as the Editor-in-Chief of the IEEE INTERNET OF THINGS JOURNAL, IEEE NETWORK, and *IET Communications*. He is a registered Professional Engineer of Ontario, Canada, a Fellow of the Engineering Institute of Canada, Canadian Academy of Engineering, and a Royal Society of Canada, a Chinese Academy of Engineering Foreign Member, and a Distinguished Lecturer of the IEEE Vehicular Technology Society and Communications Society.

Chunyan Miao (Senior Member, IEEE) received the B.S. degree from Shandong University, Jinan, China, in 1988, and the M.S. and Ph.D. degrees from Nanyang Technological University (NTU), Singapore, in 1998 and 2003, respectively.

She was an NSERC Postdoctoral Fellow with Simon Fraser University (SFU), Burnaby, BC, Canada. She is a President's Chair Professor and the Chair of the School of Computer Science and Engineering, NTU. She is the Founding Director of the Joint NTU-UBC Research Centre of Excellence in Active Living for the Elderly, Singapore's first centre focusing on AI-empowered solutions to population aging challenges. She is also the Founding Director of the Alibaba-NTU Singapore Joint Research Institute (JRI), Alibaba's first and largest JRI outside China. She was a Founding Faculty Member of the Centre for Digital Media established by The University of British Columbia, Vancouver, BC, Canada, and SFU.

Dr. Miao has received over 20 Best Paper/Innovation Awards in Artificial intelligence (AI) and real-world AI applications for her impactful research in health, aging, education, and smart services. She was awarded the Public Administration Medal (Bronze) from the President of Singapore in 2016. She is a recipient of the prestigious NRF Investigatorship Award 2018. She also holds major research funding, including the MOH National Innovation Challenge on Ageing Award 2018 and the NRF AI.SG Health Grand Challenge Award 2019. She is an Editor/Associate Editor of leading international journals, including the *International Journal of Information Technology*, IEEE TRANSACTIONS ON BIG DATA, IEEE INTERNET OF THINGS JOURNAL, IEEE ACCESS, and IEEE TRANSACTIONS ON SERVICES COMPUTING and has served as a Chair/TPC Member for international conferences, such as IEEE ICA, ICAA, and ACM KDD. She serves for various national committees, including the MOH City for All Ages and Health Tech and IMDA TechSkills Accelerator and is the Chair of the Singapore Computer Society (SCS) AI Ethics Review Committee. She was also a Tan Chin Tuan Engineering Fellow at Harvard and MIT. She is a Fellow of SCS.